Title: The Arabidopsis PHYTOCHROME KINASE SUBSTRATE2 protein is a phototropin signaling element that regulates leaf flattening and leaf positioning.

Authors: de Carbonnel M, Davis P, Roelfsema MR, Inoue S, Schepens I, Lariguet P, Geisler M, Shimazaki K, Hangarter R, Fankhauser C

Journal: Plant physiology

Year: 2010 Mar

Volume: 152

Issue: 3

Pages: 1391-405

DOI: 10.1104/pp.109.150441

Page 1

Running head : (max. 60 characters and space)

Regulation of leaf flattening and positioning by PKS2

Corresponding author:

Christian Fankhauser

Center for Integrative Genomics

University of Lausanne

Genopode Building

1015 Lausanne, Switzerland

Phone n° ++41 21 692 3941;

FAX n° ++41 21 692 3925

e-mail: christian.fankhauser@unil.ch

Journal research area most appropriate for the paper:

Signal Transduction and Hormone Action – Associate Editor Bonnie Bartel

Development and Hormone Action – Associate Editor Richard Amasino

Page 2

Title of article:

The *Arabidopsis* PHYTOCHROME KINASE SUBSTRATE 2 protein is a phototropin signaling element that regulates leaf flattening and leaf positioning.

Authors' full names:

Matthieu de Carbonnel [a], Phillip Davis [b], M. Rob G. Roelfsema [c], Shin-ichiro Inoue [d], Isabelle Schepens [a], Patricia Lariguet [e], Markus Geisler [f], Ken-ichiro Shimazaki [d], Roger Hangarter [b] and Christian Fankhauser [a]

Institutions addresses:

[a] Center for Integrative Genomics, University of Lausanne, Genopode Building, 1015 Lausanne, Switzerland (M.C., I.S. C.F.)

[b] Department of Biology, Indiana University, Bloomington, 47405, USA (P.D., R.H.)

[c] Molecular Plant Physiology and Biophysics, Julius-von-Sachs Institute for Biosciences, Biocenter, Würzburg University, Julius-von-Sachs-Platz 2, D-97082 Würzburg, Germany (R.R.)

[d] Department of Biology, Faculty of Science, Kyushu University, Ropponmatsu, Fukuoka 810-8560, Japan (S.I.I., K.I.S)

[e] Department of Plant Biology, University of Geneva, 30 Quai Ernest Ansermet, 1211 Geneva 4, Switzerland.

[f] Institute of Plant Biology, University of Zürich, Zolliker Strasse 107, 8008 Zürich, Switzerland.

Page 3 (Footnotes)

Financial sources:

This work was supported by grants from the NCCR “Plant Survival” to C.F., the Swiss National Foundation (n° 3100A0-112638 to C.F. and n° 31003A-111912 to M.G.) and by an NSF grant n° IOB0416741 to R.P.H.

Present addresses:

Isabelle Schepens: Universitätsklinik für Dermatologie, University of Bern, Freiburgstrasse, 3010 Bern, Switzerland.

Corresponding author:

Christian Fankhauser

christian.fankhauser@unil.ch

Page 4 - Abstract

In *Arabidopsis thaliana* (L.), the blue light photoreceptors phototropins (phot1 and phot2) fine-tune the photosynthetic status of the plant by controlling several important adaptive processes in response to environmental light variations. These processes include stem and petiole phototropism (leaf positioning), leaf flattening, stomatal opening, and chloroplast movements. The PHYTOCHROME KINASE SUBSTRATE (PKS) protein family comprises four members in *Arabidopsis* (PKS1 to PKS4). PKS1 is a novel phot1 signaling element during phototropism as it interacts with phot1 and the important signaling element NON-PHOTOTROPIC HYPOCOTYL 3 (NPH3), and is required for normal phot1-mediated phototropism. In this study, we have analyzed more globally the role of three PKS members (PKS1, 2 and 4). Systematic analysis of mutants reveals that PKS2 (and to a lesser extent PKS1) act in the same subset of phot-controlled responses as NPH3, namely leaf flattening and positioning. PKS1, PKS2 and NPH3 co-immunoprecipitate with both phot1-GFP and phot2-GFP in leaf extracts. Genetic experiments position PKS2 within phot1 and phot2 pathways controlling leaf positioning and leaf flattening, respectively. NPH3 can act in both phot1 and phot2 pathways, and synergistic interactions observed between *pks2* and *nph3* mutants suggest complementary roles of PKS2 and NPH3 during phot signaling. Finally, several observations further suggest that PKS2 may regulate leaf flattening and positioning by controlling auxin homeostasis. Together with previous findings, our results indicate that the PKS proteins represent an important family of phot-signaling proteins.

Introduction

Plants constantly monitor the properties of light in their natural environment to optimize light capture for photosynthesis and growth (e.g. shade avoidance and phototropism) and to time important developmental transitions (e.g. germination and flowering) (Neff et al., 2000; Briggs and Christie, 2002; Franklin and Whitelam, 2005). To do so, plants have a multitude of photoreceptors that allow them to sense changes in light period, direction, wavelength composition and intensity. The main types of photoreceptors are the red/far-red light-absorbing phytochromes and the UV-A/blue light-sensing phototropins, cryptochromes and Zeitlupe protein families (Chen et al., 2004; Jiao et al., 2007; Demarsy and Fankhauser, 2009). The signaling pathways triggered by these photoreceptors are integrated to fine-tune responses to ever-changing light environments (Casal, 2000; Franklin and Whitelam, 2004; Iino, 2006).

In *Arabidopsis*, phototropin1 (phot1) and its paralog phot2 were discovered as primary photoreceptors for blue light-induced hypocotyl phototropism and for high light-induced chloroplast avoidance movements, respectively (Liscum and Briggs, 1995; Huala et al., 1997; Jarillo et al., 2001; Kagawa et al., 2001). Subsequent studies have shown that phototropins regulate a wide set of physiological and developmental responses including chloroplast accumulation under low light, stomatal opening, leaf flattening, and phototropism of the root, inflorescence stem and petiole (Sakai et al., 2001). Thus, phototropins are proposed to optimize the photosynthetic potential of plants particularly under unfavorable environments such as extremely high light, weak illumination, and drought (Kasahara et al., 2002; Takemiya et al., 2005; Galen et al., 2007).

Phot1 and phot2 regulate these processes selectively and in a fluence-dependent manner. Phot1 mediates the chloroplast accumulation, leaf positioning and phototropic responses under very low light (Demarsy and Fankhauser, 2009). Under higher light intensities, the phot2 pathway becomes activated and acts redundantly with phot1 in these processes (Sakai et al., 2001). Phot2 also specifically controls the chloroplast avoidance response induced by high light (Jarillo et al., 2001; Kagawa et al., 2001). For stomatal opening,

phot1 and phot2 act redundantly over a broad range of light intensity (Kinoshita et al., 2001; Doi et al., 2004).

Phototropins are serine / threonine kinases belonging to the AGC family (cAMP-dependent protein kinase, cGMP-dependent protein kinase, and phospholipids-dependent protein kinase C) (Bogre et al., 2003). Two LOV (Light, Oxygen, or Voltage) photosensory domains that bind to the blue light-absorbing chromophore FMN (Flavin Mono-Nucleotide) regulate the kinase activity (Christie, 2007). Phototropin activation and early signaling events at the level of the photoreceptor itself have been extensively studied (Tokutomi et al., 2008; Demarsy and Fankhauser, 2009). However, downstream signaling is less well understood. Light-induced phot1 autophosphorylation has recently been shown to be an essential signaling event, but apart from the photoreceptor itself no direct substrate for the kinase activity has been identified *in planta* (Sullivan et al., 2008; Inoue et al., 2008b). Nonetheless, several proteins are known to interact with phot1. These include Broad-Complex, Tamtrack, Brick-à-Brack (BTB) proteins belonging to the 33-member NRL (NON-PHOTOTROPIC HYPOCOTYL 3 / ROOT PHOTOTROPISM 2 – like) subfamily, 14-3-3 proteins, and ADP-ribosylation factors (members of the Ras superfamily of GTP-binding proteins that play important roles in the assembly and disassembly of coat proteins associated with driving vesicle budding and fusion) (Motchoulski and Liscum, 1999).

Genetic experiments showed that NPH3 is required for phot1- and phot2-mediated phototropism and for phot1-controlled leaf positioning, but is not involved in stomatal opening or chloroplast movements (Inada et al., 2004; Inoue et al., 2008a). In addition, RPT2 acts in the phot1-induced phototropic response and stomatal opening but not in chloroplast relocation or phot2-induced chloroplast movements. RPT2 can associate with phot1 *in vitro* and *in vivo*, but there is no evidence for a direct interaction with phot2 (Inada et al., 2004). NPH3 is also known to interact with phot1 *in vivo*, but an interaction with phot2 has not been yet reported (Motchoulski and Liscum, 1999; Lariguet et al., 2006). Thus, phot signaling is believed to branch quickly and phot1 and phot2 appear to recruit different signaling components to trigger distinct physiological processes. NPH3

and RPT2 are proposed to mediate protein scaffolding using their protein-protein interaction domains (BTB / Pox virus and Zing finger (POZ), and coiled-coil), and by these means may provide signaling specificity via interaction with specific targets in different tissues and subcellular compartments (Celaya and Liscum, 2005). The phototropins may regulate such interactions by modifying the phosphorylation status of the signaling protein (e.g. NPH3 and 14-3-3 proteins) (Pedmale and Liscum, 2007; Sullivan et al., 2009).

The nature of phototropin-controlled responses is diverse. On the one hand, chloroplast movements and stomatal opening are rapid, cell autonomous and reversible processes. On the other hand, phototropic responses and leaf flattening are slower (a) symmetric growth processes coordinated by cell expansion and division. Such growth coordination is under tight hormonal regulation and the hormone auxin is a central regulator of phototropism (Holland et al., 2009), leaf flattening (Keller and Van Volkenburgh, 1997; Li et al., 2007; Bainbridge et al., 2008; Braun et al., 2008) and leaf positioning (Tao et al., 2008). An important task is to identify points of convergence between phototropin signaling and auxin signaling. Hypocotyl phototropism is triggered by blue light-induced auxin redistribution and signaling across the organ (Esmon et al., 2006; Holland et al., 2009). Recent reports suggest that the phototropins achieve this by directly regulating the activity of auxin transporters. First, the three main classes of auxin transporters (AUXIN RESISTANT 1 (AUX1) / like-AUX1 (LAX), PIN-FORMED (PIN) and *P*-glycoproteins (PGP)) are involved in the regulation of phototropism (Friml et al., 2002; Noh et al., 2003; Blakeslee et al., 2004; Nagashima et al., 2008; Stone et al., 2008). Second, phot1 is required for the relocalization of PIN1 upon blue light exposure (Blakeslee et al., 2004). Third, the phot-related AGC kinase PINOID (PID) is a crucial regulator of PIN1 intracellular cycling, which suggests an important role for AGC kinases in the regulation of auxin transport polarity (Michniewicz et al., 2007; Robert and Offringa, 2008). The link between the phototropins and auxin has not been firmly established in the cases of leaf flattening and leaf positioning.

NPH3 is a strong candidate to provide a link between phototropins and auxin transport. First, NPH3 acts specifically in phot-controlled processes that involve growth regulation. Second, the rice homolog of NPH3 called COLEOPTILE PHOTOTROPISM 1 (CPT1) is an essential mediator of auxin redistribution in coleoptiles during the phototropin response (Haga et al., 2005). Third, an *Arabidopsis* homolog of NPH3 named MACCHIBOU 4 / ENHANCER OF PINOID / NAKED PINS IN YUC MUTANTS (MAB4 / ENP / NPY1) is involved in organogenesis synergistically with PID by controlling PIN1 localization in embryo and inflorescence stems (Cheng et al., 2007; Furutani et al., 2007). However, beyond these correlative observations, the mechanisms of auxin transport regulation by phototropin signaling remains poorly understood (Holland et al., 2009).

PHYTOCHROME KINASE SUBSTRATE (PKS) proteins were initially identified as phytochrome signaling components that regulate developmental processes such as de-etiolation and growth orientation of roots and hypocotyls (Fankhauser et al., 1999; Lariguet et al., 2003; Khanna et al., 2006; Boccalandro et al., 2008; Molas and Kiss, 2008; Schepens et al., 2008). PKS1, PKS2 and PKS4 interact with phyA and PKS1 is phosphorylated by phyA *in vitro* (Fankhauser et al., 1999; Lariguet et al., 2003; Schepens et al., 2008). Recently, we have shown that PKS1 also interacts with phot1 and NPH3 *in vivo*, and is required for phot1-mediated root and hypocotyl phototropism (Lariguet et al., 2006; Boccalandro et al., 2008). The importance of PKS proteins for phototropism prompted us to test their involvement in phototropin-mediated responses more globally. Here, we show that PKS2 acts in phot1 and phot2 signaling pathways controlling leaf positioning and leaf flattening but not chloroplast movements and stomatal opening. Interestingly, PKS2 and NPH3 selectively control phot-mediated growth responses and interact genetically. Several lines of evidence including auxin transport assays in mesophyll protoplasts suggest that PKS2 may regulate these developmental light responses by modulating auxin homeostasis.

Results

PKS2 and PKS1 control leaf flattening

Since *PKS1/2/4* are required for phototropism and PKS1 is associated with phot1 *in vivo* (Lariguet et al., 2006; Boccalandro et al., 2008), we used a genetic approach and analyzed leaf flattening, leaf positioning, chloroplast movements and stomatal opening in the *pks* mutants to determine whether members of the *PKS* gene family are global regulators of phot signaling. Our analyses excluded *PKS3* for which no null mutants were available. Since phot1 and phot2 can act redundantly in these processes we also included *phot1pks* and *phot2pks* mutants in our experiments (Sakai et al., 2001; Takemiya et al., 2005; Inoue et al., 2008a). These mutants also enabled us to determine epistatic interactions between *pks* and *phot* mutations and to position the PKS proteins within phot1 and / or phot2 pathways.

Under our experimental conditions (80 µmol m^{-2} s^{-1} WL; 16 hours light photoperiod), phot1 and phot2 mediated leaf flattening redundantly because leaves curled only in the *phot1phot2* double mutant and not in the single mutants (Figure 1A). Leaves of *pks1pks2pks4* and *phot2pks1pks2pks4* mutants were mildly but significantly less flat when compared to wild type and *phot2*, respectively (p-value<0.01; Figure 1A). The *phot1pks1pks2pks4* mutant showed a more visible leaf epinasty phenotype characterized by the downwards curling of laminas near the margin (Figure 1A). Thus, an effect of *PKS* loss of function was more visible in plants that had an impaired phot1 pathway. To further study the role of *PKS1/2/4* in leaf flattening we crossed *pks* mutants with the phot1-signaling mutant *nph3* that displays impaired phot1-mediated leaf flattening and positioning (Inoue et al., 2008a). Interestingly, *PKS1/2/4* loss of function in the *nph3* background increased leaf epinasty in a synergistic manner and *nph3pks1pks2pks4* phenocopied *phot1phot2* (Figure 1A). Analysis of double and triple *nph3pks* mutants revealed a predominant role for *PKS2* and a minor role for *PKS1*, while *PKS4* did not seem to contribute to leaf flattening (Supplemental Figures 1A and 1C). Taken together, these results indicate that PKS2 and PKS1 act in the phot2 pathway controlling leaf

flattening (Figure 1B). Importantly, the comparison of leaf curling between *phot1phot2* and *phot1pks1pks2pks4* suggests that phot2 signaling is not totally abolished in *pks1pks2pks4* mutants (Figure 1).

Under our experimental conditions, the *nph3* mutant was more epinastic than *phot1* and had an intermediate phenotype between *phot1* and *phot1phot2*. This observation suggested to us that NPH3 also plays a significant role in the phot2 pathway. To test this hypothesis we crossed *nph3* with *phot1* and *phot2*. To our surprise, the *nph3phot1* mutant displayed much stronger leaf epinasty than *nph3* and resembled the *phot1phot2* mutant while no increased leaf curling was observed in *nph3phot2* plants (Figure 1A). These results indicate that NPH3 acts in both phot1 and phot2 pathways, and has a crucial role in the phot2 pathway under our experimental conditions (Figure 1B). Finally, we noticed that *PHOT2* loss of function generated flatter leaves in the backgrounds tested (wild type, *pks1pks2pks4* and *nph3*; p-value<0.01), suggesting that phot2 might negatively regulate the phot1 pathway (Figure 1B).

PKS2 and PKS1 control leaf positioning

To investigate the role of the *PKS* in phot-mediated leaf positioning we used an experimental setup based on the protocol of Inoue and co-workers (Inoue et al., 2008a). Plants were first grown under standard WL conditions to allow initial development of first true leaves (growth stage 1.01; (Boyes et al., 2001)). The developing young true leaves were then subjected for several days (until they reached growth stage 1.04) to either a low blue light (LBL) fluence rate that activated only the phot1 pathway, or an intermediate blue light (HBL) fluence rate that triggered both phot1 and phot2 pathways (Inoue et al., 2008a). The angle between the hypocotyl and the petiole of true leaves was measured and used as an indication of leaf positioning.

Among the *pks* single mutants tested, *pks2* displayed a mild but significant phenotype under both LBL and HBL: *pks2* petioles had less erect petioles (reduced hyponasty) compared to wild type. Consistent with leaf flattening data, the *pks2-2* allele generated a

stronger phenotype than the *pks2-1* allele (Figure 2A). This may be due to the presence of small amounts of truncated PKS2 protein in *pks2-1*, while *pks2-2* is a complete knock-out (Supplemental Figure 1B). The leaf positioning phenotype of *pks2* did not correlate with changes in circadian movements (Mullen et al., 2006), as might be suggested by the circadian expression of *PKS2* (Lariguet et al., 2003; data not shown). Leaf positions of *pks4* and wild-type plants were undistinguishable. However, *pks1* plants showed a very mild but significant phenotype (p-value<0.01) that was additive with the *pks2* phenotype (as shown when comparing *pks1pks2pks4* with *pks2*) (Figure 2A). Thus similarly to leaf flattening, *PKS2* and to a lesser extent *PKS1* are involved in leaf positioning. To further study the role of PKS2, we analysed the effects of *PKS2* gain-of-function. Two independent *PKS2* over-expressing lines that expressed approximately ten times more PKS2 protein (Lariguet et al. 2003; data not shown) displayed the opposite phenotype to *pks2* and had more erect leaves (enhanced hyponasty) compared to wild-type plants (Figure 2B). Taken together, these results indicate that PKS2 plays a significant role in leaf positioning.

Under our LBL conditions, *phot1* resembled *phot1phot2* indicating that the phot2 pathway was not activated. As previously reported, *nph3* phenocopied *phot1* supporting an essential role for NPH3 in the phot1 pathway under LBL (Figure 3A) (Inoue et al., 2008a). Under HBL conditions, the phot2 pathway was activated because the *phot1* mutant was able to elevate its petioles while strong downwards petiole curling (petiole epinasty) was observed in the *phot1phot2* mutant. Under HBL, the *nph3* mutant showed a slightly stronger leaf positioning defect than *phot1* (Figure 3A), and *nph3* laminas were also slightly epinastic while *phot1* laminas were always positioned in a horizontal plane (Figure 3C). As in the case of leaf flattening, these results suggest a role for NPH3 in the phot2 pathway. Epistasis results between *nph3* and *phot* mutants revealed again an important role for NPH3 in the phot2 pathway. Indeed, *nph3phot1* resembled *phot1phot2* while *PHOT2* loss of function did not increase petiole epinasty in the *nph3* background (Figures 3A and 3C). Thus, these genetic and photobiological experiments suggest that NPH3 plays a crucial role in the phot1 pathway under LBL, and an increasingly more important role in the phot2 pathway under higher fluence rates of BL (Figure 3D).

phot1pks2, *phot2pks2* and *nph3pks2* mutants were analyzed to position *PKS2* in the phot pathways controlling leaf positioning. Under both HBL and LBL *phot1* appeared epistatic over *pks2*, while *pks2* was epistatic over *phot2* (Figure 3B). These data indicate that PKS2 acted predominantly in the phot1 pathway (Figure 3D). Interestingly, while *phot1pks2* and *phot1* leaf positions were similar, *phot1pks2* laminas were clearly more curled than in *phot1* and *pks2* under HBL (Figure 3C). This observation is consistent with a role for PKS2 in the phot2 pathway controlling leaf flattening (Figure 1B). It also supports the conclusion that PKS2 can act in two distinct phot signaling pathways during two different leaf developmental processes, namely in the phot1 pathway controlling leaf positioning and in the phot2 pathway controlling leaf flattening (Figures 1B and 3D).

Under LBL, *nph3* was epistatic over *pks2* which is not surprising given that *nph3* fully controls leaf positioning under this fluence rate (Inoue et al., 2008a; Figure 3A). Interestingly under HBL *nph3* and *pks2* mutations interacted synergistically and the *nph3pks2* mutant essentially resembled *phot1phot2* (Figures 3B and 3C). Such genetic interaction is consistent with the interpretations of epistasis data obtained independently for *NPH3* and *PKS2*. Indeed, under HBL NPH3 played an essential role in the phot2 pathway and a significant role in the phot1 pathway. Given that PKS2 appeared to contribute partially to the phot1 pathway, knocking out *PKS2* in a sensitized background where phot1 signalling is strongly impaired and phot2 signalling is completely abolished (such as the *nph3* background) may result in a synergistic increase of the phenotype (Figure 3D). Finally, that *pks2nph3* closely resembled *phot1nph3* (and *phot1phot2*) further indicates a significant role for PKS2 in the phot1 pathway (Figure 3C).

PKS2, PKS1 and NPH3 are associated with both phot1 and phot2 in leaves

Our genetic results indicate that NPH3 and PKS2 can act in both phot1 and phot2 pathways to control leaf developmental processes. Thus, to further investigate the role of these two proteins as phot signaling elements, we decided to check whether they were

associated with phot1 and phot2 in leaves. We also included PKS1 in those experiments because *PKS1* was shown to act additively with *PKS2* in leaf flattening and positioning.

Previously, we showed that PKS1 was tightly associated with the plasma membrane in etiolated seedling, as is the case for NPH3 and phot1 (Lariguet et al., 2006). Here, we analyzed PKS2 proteins extracted from the aerial parts of plants grown for 14 days on ½ MS agar under 100 µmol m^{-2} s^{-1}. We found that PKS2 was not present in the cytosolic fraction after ultracentrifugation, but co-fractioned with phot1, phot2, NPH3, PKS1 and a plasma membrane-associated protein fused to GFP (GFP-LTi6b; (Cutler et al., 2000)) in insoluble microsomal pellets and was similarly released into solution by detergent treatment (Sakamoto and Briggs, 2002; Lariguet al., 2006; Supplemental Figure 2). To test whether these proteins were also associated *in vivo*, we immunoprecipitated GFP-tagged phot1, phot2 or LTi6b and analyzed by western blotting the immunoprecipitated material. PKS2, PKS1 and NPH3 co-immunoprecipitated with phot1-GFP and phot2-GFP, but not with GFP-LTi6b, indicating that PKS2, PKS1 and NPH3 were associated with phot1 and phot2 *in vivo* (Figure 4). It is relevant to point out that phot1-GFP and phot2-GFP were expressed under the control of their respective promoters and at similar levels to the endogenous protein, supporting the notion that the protein-protein associations reported here are physiologically meaningful (Sakamoto and Briggs, 2002; Kong et al., 2006).

PKS1/2/4 and NPH3 are not required for normal chloroplast movements or stomatal opening

We have shown that PKS2 and PKS1 regulate leaf flattening (Figure 1) and leaf positioning (Figure 2). Genetic and molecular data indicate that they can act in both phot1 and phot2 pathways. To test whether *PKS1/2/4* are global regulators of phot-mediated processes, we analyzed BL-induced stomatal opening and chloroplast movements in *pks1pks2pks4, phot1pks1pks2pks4* and *phot2pks1pks2pks4* mutants.

To study chloroplast movements, we measured blue-light-induced change in red light transmittance of leaves. This method provided an indirect but quantitative means to monitor chloroplast movements into the accumulation (low light response) and avoidance (high light response) positions (Inoue and Shibata, 1973; Trojan and Gabrys, 1996; DeBlasio et al., 2003). As previously reported, phot1 and phot2 controlled redundantly the accumulation response while only phot2 mediated the avoidance response (Figure 5B; Sakai et al., 2001). *pks1pks2pks4* plants showed no signs of impaired chloroplast movements (Figure 5A), and *phot1pks1pks2pks4* and *phot2pks1pks2pks4* looked essentially like *phot1* and *phot2,* respectively (Figure 5C). These results clearly show that *PKS1/2/4* did not play important roles in phot1 or phot2 pathways mediating the low light (accumulation) response or in the phot2 pathway controlling the high light response. *NPH3* was previously shown to be dispensable for chloroplast movements (Inada et al., 2004). Under our experimental conditions, the epinastic *nph3* and *nph3pks1pks2pks4* mutants also showed normal chloroplast movements indicating that *NPH3* and *PKS1/2/4* did not act redundantly in this process (Figure 5D).

To test phot-mediated stomatal opening, we applied blue light onto epidermal peels obtained from rosette leaves. We superimposed red light in the assay because red light increased the blue light response of guard cells (Shimazaki et al., 2007). Red light alone did not induce stomatal opening in wild type or mutants (Figure 5E). However, the addition of blue light caused a two- to three-fold increase in the width of stomatal pores in wild type. Under these conditions phot1 and phot2 redundantly controlled the response (Figure 5E) (Kinoshita et al., 2001). We did not detect significant reductions in stomatal aperture in *pks1pks2pks4*, *phot1pks1pks2pks4* or *phot2pks1pks2pks4* mutants indicating that *PKS1/2/4* were not required for phot1 or phot2 signaling during stomatal opening (Figure 5E). As for chloroplast movements, the epinastic *nph3* and *nph3pks1pks2pks4* mutants had functional guard cells meaning that *PKS1/2/4* did not act redundantly with *NPH3* during BL-induced stomatal opening (Figure 5E; Inada et al., 2004). Taken together, our genetic experiments show that PKS1/2/4 are not global regulators of phot signaling. They appear to specifically regulate with NPH3 the phot-mediated BL responses that involve growth and development (Figures 1 and 3) (Motchoulski and

Liscum, 1999; Inada et al., 2004; Lariguet et al., 2006; Boccalandro et al., 2008; Inoue et al., 2008a).

Contribution of leaf flattening and positioning to plant growth under intermediate WL fluence rates

Takemiya and co-workers have shown that under low photosynthetically active radiation (PAR - 25 μmol m^{-2} s^{-1} WL), phot1 and phot2 promote photosynthesis and plant growth by driving chloroplast positioning into the accumulation position, opening stomata and flattening leaves (Takemiya et al., 2005). In the same study under higher PAR (70 μmol m^{-2} s^{-1} WL), *phot1phot2* mutants displayed flat leaves and normal plant growth. These results suggested that phots mediate plant growth enhancement specifically in low light environments. However, under our experimental conditions (80 μmol m^{-2} s^{-1} WL) *phot1phot2* displayed highly curled leaves (Figures 1). The different phenotype reported for *phot1phot2* by Takemiya and colleagues and ourselves could be due to a number of variations in the experimental procedure such as photoperiod, the light source, growth stage and humidity (Takemiya et al., 2005). The fact that chloroplast movement and stomatal opening were also abolished in *phot1phot2* even under high fluence rates of blue light encouraged us to test whether phot-deficient plants also suffered reduced plant growth under intermediate PAR (75 and 150 μmol m^{-2} s^{-1} WL). We included the *nph3pks1pks2pks4* mutant to specifically study the contribution of leaf flattening and positioning in plant growth.

Under 150 μmol m^{-2} s^{-1} WL, cotyledons and true leaves of *phot1phot2* mutant plants displayed strong epinasty throughout plant development. In parallel, we observed a gradual decrease in green tissue fresh weight of *phot1phot2* relative to wild type plants over a ten-day period (Figure 6 A-C) indicating that the phot-mediated responses played a crucial role in plant growth. The cotyledons and true leaves of *nph3pks1pks2pks4* plants were very epinastic and resembled *phot1phot2* throughout plant development. Interestingly, *nph3pk1pks2pks4* plants accumulated significantly more mass than *phot1phot2* in early stages of growth (similar to *nph3*), suggesting that functional

chloroplast movements and stomatal opening may have significantly contributed to plant growth (Figure 6 A-C). However, mass accumulation in *nph3pks1pks2pks4* subsequently dropped in later stages of growth and reached similar levels to *phot1phot2*. This drop correlated with a significantly stronger leaf epinasty in *nph3pks1pks2pks4* compared to *phot1phot2* (Supplemental Figure 4B). Taken together, these results indicate that leaf flattening is very important for plant growth even under favorable light conditions. Similar results were obtained for plants grown under 75 μmol m^{-2} s^{-1} WL (Supplemental Figure 3).

We reasoned that diminished plant growth observed in epinastic mutants could be the consequences of reduced light capture leading to reduced photosynthesis and /or a basal defect in leaf expansion. To address these hypotheses we analyzed the morphology and physiology of whole leaves. Morphology studies were done on leaf number five of plants that had reached growth stage 1.11 (Figure 6C and Supplemental. Figure 4A) because this leaf was well expanded and probably had a high contribution to plant vegetative vigor (Kerstetter and Poethig, 1998). The area of light interception by *nph3pks1pks2pks4* and *phot1phot2* leaves was three-fold smaller than wild type or *pks1pks2pks4* leaves. *nph3* showed a two-fold reduction (Figure 7A). The total area of *nph3pks1pks2pks4* and *phot1phot2* leaves was also smaller than wild type (50 % of wild type size) and *nph3* also showed a 30 % decrease in size (Figure 7B). Similar results were obtained for plants grown under 75 μmol m^{-2} s^{-1} WL (data not shown). Thus, slower plant growth in the mutants correlated with both reduced light capture and reduced leaf expansion. One simple interpretation of this data is that plants had smaller leaves because of reduced photosynthetic activity and overall growth as a consequence of reduced light capture. This hypothesis is consistent with the fact that epinastic mutants also developed more slowly than wild type-like plants (Supplemental Figure 4B). Nonetheless, one cannot exclude the possibility that basal developmental defects also hindered leaf expansion and overall plant growth in a photosynthesis-independent fashion. To investigate these possibilities we first measured transpiration and photosynthetic activity of whole leaves using gas exchange assays.

Analysis of RL- and BL-induced transpiration in whole leaves showed that all mutants except *phot1phot2* responded to the addition of blue light (Figure 7C). This result indicates that BL-induced stomatal opening data previously obtained for isolated cells were meaningful in a whole-leaf context (Figure 5E). Interestingly, this BL-induced enhancement of transpiration (i.e. the slope of the curve upon BL treatment) was significantly reduced in the epinastic *nph3pks1pks2pks4* mutant compared to *nph3*, *pks1pks2pks4* and wild type leaves, and this was not due to lower stomatal density (Figures 7C and 7D). This indicates that leaf curling had an effect on leaf gas exchange. Since stomatal opening is a limiting step for CO_2 assimilation by photosynthesis, we asked whether the epinastic *nph3pks1pks2pks4* leaves also showed reduced photosynthetic activity (Roelfsema et al., 2002; Roelfsema and Hedrich, 2005). Using the gas exchange assay we observed that this was indeed the case (Supplemental Figure 5). Although these results did not enable us to determine whether leaf epinasty had a primary consequence on stomatal opening potential or on photosynthesis itself, they nonetheless correlate with the slower growth of the epinastic *nph3pks1pks2pks4* mutant. These observations support the notion that leaf morphological changes in epinastic mutants affect overall photosynthesis and growth. However, it is difficult to determine the means by which leaf curling impairs photosynthesis.

To further test the hypothesis that growth of *nph3pks1pks2pks4* and *phot1phot2* epinastic plants suffered because of basal defects in development, we analyzed the pattern and size of leaf epidermal cells. The epidermis is a particularly relevant tissue to analyze because it restricts growth (Savaldi-Goldstein and Chory, 2008). No significant differences in epidermal cell size of either leaf number five abaxial or leaf number six adaxial surfaces could be identified in *nph3pks1pks2pks4* compared to wild type, *pks1pks2pks4* or *nph3* (Supplemental Figure 6A-B). Furthermore, the average size of pavement cells was similar from apex to base and from margin to midvein in both epinastic and wild type plants indicating that these leaves were not significantly delayed in their development (data not shown; (Donnelly et al., 1999; Autran et al., 2002)). However, the abaxial epidermis of curled leaves number five had fewer cells than wild type leaves (Supplemental Figure 6C). Thus, the reduced leaf size in both *nph3pks1pks2pks4* and

phot1phot2 epinastic mutants may be due to reduced cell division rather than lower cell expansion. However, it is difficult to determine yet whether such cellular defects are the cause for downwards leaf curling.

A possible link between PKS2 and auxin transport

Previously, we showed that the *pks* mutants, and in particular *pks4*, showed abnormal hypocotyl growth orientation in red and far-red light (Schepens et al., 2008). Moreover, *pks4* mutants show slower gravitropic-reorientation in dark-grown hypocotyls suggesting that PKS proteins may play a general role in the control of growth orientation (Schepens et al., 2008). We thus tested whether PKS2 played a role in petiole positioning that cannot be attributed to phot signaling by analyzing seedlings grown in red light. Interestingly, *pks2* petioles were slightly more horizontal than the wild type while *PKS2* over-expressing plants had the converse phenotype with more elevated leaves (Figure 8A). This data indicates that PKS2 modulates leaf positioning under conditions where the phototropins are not expected to play a role given that they specifically absorb blue and not red light.

The expression of *PKS1*, *PKS2* and *PKS4* has been described in young etiolated seedlings and seedlings treated for a few days with light. *PKS1* and *PKS4* are both expressed in the hypocotyl elongation zone, which correlates with their involvement in the control of hypocotyl growth orientation (Lariguet et al., 2003; Schepens et al., 2008). Similarly only *PKS1* is expressed in the root elongation zone and this is the only member of the *PKS* family that is required for negative hypocotyl phototropism (Boccalandro et al., 2008). *PKS2* is expressed in hypocotyls and cotyledons of young seedlings but its expression in older light-grown seedlings has not been analyzed (Lariguet et al., 2003). The role of *PKS2* in leaf flattening and positioning prompted us to analyze its expression in leaves using *PKS2* promoter driven GUS lines. *PKS2* was expressed quite broadly in leaves but the strongest expression was observed on edges of the laminas (Figure 8B). This correlates with the leaf curling that was also most obvious near the leaf margins in

phot1pks mutants (Figure 1A). Moreover it is noteworthy that the auxin reporter gene *DR5:GUS* was also mostly expressed in the leaf margin area (Figure 8B).

The similarity of expression between *PKS2* and *DR5* in the leaves and the finding that *PKS* genes are involved in the control of asymmetric growth responses under different conditions suggested that PKS proteins might modulate auxin transport (Lariguet et al., 2006; Boccalandro et al., 2008; Schepens et al., 2008). To test this hypothesis we analyzed auxin accumulation using the well-established mesophyll protoplast system (Geisler et al., 2005). The accumulation of auxin was reduced in the *aux1* mutant, which is consistent with the role of AUX1 as an auxin influx carrier (Figure 8C). Both in *pks1* and *pks2*, but most significantly in *pks1pks2* double mutants, we found an enhanced accumulation of auxin in mesophyll protoplasts (Figure 8C). This result indicates that PKS1 and PKS2 either inhibit influx of auxin into the protoplast or promote auxin efflux, either of which would result in increased accumulation of auxin in the *pks1pks2* double mutant (Figure 8C).

Discussion

Using a systematic genetic approach we found that PKS1/2/4 are not required for blue-light-regulated chloroplast movements or stomatal opening (Figure 5), but that PKS1 and PKS2 act with NPH3 as important regulators of leaf flattening and positioning (Figures 1-3). PKS1 is a phot1-associated protein that plays important roles in phot1-mediated tropisms (Lariguet et al., 2006; Boccalandro et al., 2008). Our epsistasis and immunoprecipitation results expand the role of PKS1 and PKS2 to the phot2 pathway during leaf flattening and positioning (Figures 1-4). We have also observed a good correlation between the expression pattern of *PKS* genes and the organ in which they play the most predominant function. For instance, *PKS1* is highly expressed in roots and is essential for root phototropism while *PKS2* is expressed in leaves and controls leaf flattening (Figures 1-3, 6 and 8; Lariguet et al., 2003; Boccalandro et al., 2008). This may represent an example of functional specialization of *PKS1* and *PKS2*, which is a common phenomenon for paralogous gene pairs that arose during the last *Arabidopsis* whole gene duplication (Duarte et al., 2006).

NPH3 is required both for phot1 and phot2-mediated phototropism (Motchoulski and Liscum, 1999). NPH3 was recently shown to be involved in phot1-mediated leaf flattening and positioning, and our results show that NPH3 also acts in the phot2 signaling branch regulating these light responses (Figures 1 and 3) (Inoue et al., 2008a). NPH3 and PKS proteins thus appear to play important roles exclusively in phot-controlled developmental processes. It is possible that phototropins utilize different protein families with distinct biochemical properties to control different light responses. However, it is surprising that RPT2 (a member of the NPH3 family) is also required for stomatal opening (Inada et al., 2004). Thus, while PKS function seems restricted to asymmetric growth processes, the NRL family may have more versatile functions during phototropin signaling (Inada et al., 2004).

Phot1 and phot2 represent the initial step in phototropin signaling because blue light induced processes are abolished in the *phot1phot2* double mutant (Briggs and Christie,

2002). It is not clear yet whether the four PKS proteins play an essential role in the pathway controlling leaf flattening and positioning because the *pks1pks2pks3pks4* mutant is not yet available. The fact that root phototropism is abolished in the *pks1* mutant (*pks1* phenocopies the *phot1* mutant) indicates that PKS proteins might accomplish specific functions during phot signaling (Boccalandro et al., 2008). Two basic models can explain the synergistic interactions observed between *pks* mutants and *nph3* during leaf flattening and positioning. In the first one, both gene products act in parallel pathways controlling these growth responses in leaves. In the second model, partial knock-out of different steps of the same pathway can also result in synergistic aggravation of the leaf phenotype. Analysis of the *pks* quadruple mutant will allow us to determine whether the PKS proteins control a key step in this signaling pathway. The presence of NPH3, PKS1 and PKS2 in phot1-GFP and phot2-GFP immunoprecipitates is certainly consistent with them acting in the same pathway (Figure 4) (Lariguet et al., 2006; Boccalandro et al., 2008; Molas and Kiss, 2008; Schepens et al., 2008).

There is a growing body of literature that functionally link phototropin-mediated asymmetric growth processes with auxin function (Esmon et al., 2006; Whippo and Hangarter, 2006). For instance in hypocotyls, phot1 has been shown to control blue light induced PIN1 relocalisation in response to lateral blue light (Blakeslee et al., 2004). Auxin transport by PGP19, PIN3 and AUX1, as well as auxin-dependent transcription are required for normal phototropism (Friml et al., 2002; Tatematsu et al., 2004; Stone et al., 2008). Although in the case of leaf flattening a direct connection between phototropin and auxin signaling has not been yet established, several genetic and pharmacological experiments provide evidence that leaf flattening is also regulated by auxin homeostasis and signaling (Keller and Van Volkenburgh, 1997; Li et al., 2007; Bainbridge et al., 2008). Analogous scenarios can be envisaged where in hypocotyls the phototropins coordinate asymmetric growth while in the leaves the same photoreceptors coordinate symmetric growth of the lamina to ensure its flatness (Poethig, 1997; Whippo and Hangarter, 2006).

The role of phototropins in the control of petiole positioning may also be analogous to the situation in hypocotyls because in both cases the phototropins control asymmetric growth responses resulting in optimal positioning of the leaves to absorb light. Moreover, in both cases several photoreceptors control the growth response and several hormones including auxin have been shown to play a prominent role (Lariguet and Fankhauser, 2004). For example the phytochromes, auxin synthesis and auxin transport are required to control leaf positioning in response to low red/far-red ratios indicative of vegetational shade (Tao et al., 2008). Low light conditions also trigger a more erect leaf position requiring cryptochromes, phytochromes, auxin and polar auxin transport (Millenaar et al., 2009). Importantly, phototropin mutants in the presence of blue light have strongly epinastic petioles, which clearly links this growth response to phototropin activity (Figures 3 and 8) (Inoue et al., 2008a). The function of the PKS proteins in petiole orientation is thus noteworthy given that these proteins modulate growth responses downstream of both the phototropins and the phytochromes suggesting that they may affect a process common to both light signaling pathways such as auxin signaling and/or homeostasis (Figure 3 and 8) (Lariguet et al., 2006; Boccalandro et al., 2008; Molas and Kiss, 2008; Schepens et al., 2008).

Several findings connect NPH3 and PKS proteins with auxin signaling. In rice with a mutation in the *NPH3*-ortholog *CPT1*, auxin relocalization no longer occurs in response to unilateral blue light indicating that CPT1 acts upstream of asymmetric auxin distribution (Haga et al., 2005). Also, other NRLs are involved in auxin-regulated organogenesis (Cheng et al., 2007; Furutani et al., 2007; Cheng et al., 2008). Taken together these studies suggest that NRL proteins function in auxin-mediated growth processes. Phenotypic analyzes of *pks* mutants in phytochrome and phototropin-mediated responses indicate that these genes are primarily required for asymmetric growth responses (gravitropism and phototropism) (Lariguet et al., 2006; Boccalandro et al., 2008; Molas and Kiss, 2008; Schepens et al., 2008). The function of PKSs and NPH3 in the same subset of phot-mediated responses, their presence in the same complex *in vivo* and the synergistic genetic interaction between *pks* and *nph3* during leaf flattening support the notion that these proteins are required for a subset of auxin-mediated growth

responses (Figures 1-5). Also, *phot1* loss of function generated a similar effect to *pks* loss of function in the *nph3*-sensitized background (Figures 1 and 3). A similar genetic interaction was observed between *NPY1* and *PID1*, homologs of *NPH3* and *PHOT1* respectively (Cheng et al., 2007, 2008). Taken together, these results indicate that the PKS protein family is part of a genetic framework including NRLs and AGC kinases (Robert and Offringa, 2008).

Our data suggest that the PKS proteins may act in this framework at the level of auxin signaling and/or homeostasis to control leaf flatness (Figure 8). The expression pattern of *PKS2:GUS* in leaves is rather broad but strongest at the leaf margins (Figure 8B). This correlates with the strong curling at the edge of the leaf lamina in *phot1pks* quadruple mutants (Figure 1). In addition, this expression pattern is similar to the auxin reporter construct *DR5:GUS* (Figure 8B). Moreover, in comparison to the wild type, auxin accumulation was enhanced into *pks1*, *pks2* and *pks1pks2* mutant mesophyll protoplasts whereas auxin accumulation was reduced in protoplasts of the *aux1* influx carrier mutant (Figure 8C). The stronger auxin transport phenotype in *pks1pks2* compared with the *pks* single mutants correlates with the enhanced leaf flattening phenotype of *pks1pks2nph3* compared to *pks2nph3*. (Figure S1). This finding is consistent with either a role of PKS proteins as inhibitors of auxin influx or positive regulators of auxin efflux. Although they do not contain any known membrane-anchor motifs, PKS1 and PKS2 are associated with the plasma membrane (Figures 4 and S2) (Lariguet et al., 2006). One attractive hypothesis is thus that they could modulate the activity of proteins directly involved in auxin transport. Importantly AUX1 and members of its family of auxin influx carriers have recently been shown to control leaf flatness (Keller and Van Volkenburgh, 1997; Li et al., 2007; Bainbridge et al., 2008). However while in *aux1* mesophyll protoplasts auxin accumulation was reduced the opposite was found in *pks1pks2* protoplasts. Future studies are thus needed to uncover the mechanisms underlying auxin-mediated leaf flattening and how this is modulated by PKS proteins and phototropin signaling.

Material and Methods

Plant material

The following mutants used in this study were described elsewhere: *pks1-1*, *pks2-1*, *pks4-1* single and triple mutants (Lariguet et al., 2006), *phot1-5* (Huala et al., 1997) , *phot2-1* (Kagawa et al., 2001), *nph3-6* (Motchoulski and Liscum, 1999), *gl1-1* (Oppenheimer et al., 1991) and *aux1-22* (Roman et al., 1995). Unless specified otherwise, the *pks2-1* allele was used in this study (Lariguet et al., 2003). The *pks2-2* allele has a T-DNA insertion in the 113th codon and *pks2-2* plants showed no *PKS2* transcript on a northern blot. To genotype *pks2-2* plants we used CF338 [5'-CAT TTG GAC GTG AAT GTA GAC AC-3'] and AH022 [5'-CCC AAA GCC CAT TAA CGA CC-3']) to detect the T-DNA and a second pair (CF359 [5'-TCG AAC ACA CGC ATC TGC AG-3'] and AH022) to test for homozygosity. *phot1-5pks1-1pks2-1pks4-1, phot2-1pks1-1pks2-1pks4-1, nph3-6/pks1-1/pks2-1/pks2-2/pks4-1, nph3-6phot1-5* and *nph3-6phot2-1* mutants were obtained by crossing. In the F2 generation, plants bearing trichomes were preferentially selected to allow better phenotype comparisons as the *glabrous* mutation may affect leaf shape. *phot1-5phot2-1* was obtained by crossing *phot1-5phot2-1gl1-1* with *phot2-1* and genotyping in the F2 generation. All alleles used in this study are in the *Arabidopsis thaliana* (L.) Columbia-O background. Conditions of plant growth varied depending on the physiology experiment. For plants grown on soil (a blend of weakly decomposed white sphagnum peat and clay; type GS90-FAI11, Einheitserde, Germany) in a growth chamber the conditions were: 16 / 8 hrs light / dark cycle (white light source provided by a combination of Coolwhite (L36W/20) and Limilux ® Warmwhite (L36W/830) Osram fluorescent tubes), 20.5 ± 1°C and 55-75% relative humidity. For plants grown on 0.7% (w/v) agar (Sigma; Prod. No. A1296) supplemented with ½ strength MS (Duchefa Biochemie; Prod- No. M0222.0010) pH 5.7, seeds were surface-sterilized (3 mins in 70% (v/v) ethanol plus 0.05% (v/v) Triton X-100, then 10 mins in 100% (v/v) ethanol, then rinsed with sterile distilled water) and incubated in phytotron (continuous WL, 22°C). In all conditions, plants were stratified (4°C, darkness) for three days before incubation. Light intensities were determined with an International Light IL1400A photometer (Newburyport, MA) equipped with an SEL033 probe with appropriate light filters.

Growth stages were defined according to (Boyes et al., 2001) and the age of plants was noted as "days after incubation" (dai) under light.

Leaf flattening experiments

Our growth conditions differed from the ones used by Takemiya and colleagues (Takemiya et al., 2005). Approximately 50 seeds were plated on agar in Petri dishes and placed under 100 ± 10 $\mu mol.m^{-2}.s^{-1}$ continuous white light (WL) in a phytotron. After 10 dai when wild-type plants reached growth stage 1.04 plants were transplanted onto soil. Plants were then grown for 15-16 more days in a growth chamber under 80 ± 8 $\mu mol\ m^{-2}\ s^{-1}$ WL until wild-type plants reached growth stage 1.10-1.11. Trays were shuffled around to minimize the influence of microclimates in the growth chamber. The lamina of the 5^{th} rosette leaf was detached from the petiole, placed on its abaxial side on wet white whatman paper, and photographed from above using a Canon PowerShot A640 digital camera (representing curled leaf projections area). The lamina was then artificially flattened by making one or two small sections in the margin, uncurled, and gently pressed onto wet whatman paper under transparent plastic sheet to keep lamina flat by capillarity. The leaf was then photographed from above (representing total projection area). Projection areas were selected using the magic wand tool from the Adobe Photoshop Elements 4.0 software and measured using imageJ software (http://rsb.info.nih.gov/ij/). Leaf flattening index is the ratio of curled to total projection areas. In Statistical tests, a Student T-test with two-tailed distribution and two-sample unequal variance was used.

Leaf positioning experiments

Measurement of petiole positioning was based on the protocol of Inoue et al. (2008a) with many modifications. Soil was placed in 90 mm × 15 mm bacteria culture Petri dishes with five punched holes at their bottom, and the surface was evened. Dishes were then placed in trays and the soil was imbibed by adding water from below. Approximately 300 seeds were sown on each dish and stratified for three days to induce uniform germination. At 8:30 am, the trays covered with a transparent plastic dome were incubated in a growth chamber under 130 ± 10 $\mu mol\ m^{-2}\ s^{-1}$, 16 hrs light photoperiod. The domes were removed after 36 hours once the seeds had germinated and plants were

grown typically for 9 days until reaching growth stage 1.01. At 8:30 am on the 9th day, seedlings were transferred to LED incubators (22°C, continuous light) under 50 µmol m^{-2} s^{-1} RL plus 0.4 µmol m^{-2} s^{-1} BL, or RL 50 µmol m^{-2} s^{-1} plus 5.0 µmol m^{-2} s^{-1} BL and the first true leaves were let to develop for five days and eight hours. Between 5:30 pm and 8:00 pm on the 5th day of light treatment, whole Petri dishes were photographed from above using a camera stage, and individual plants were photographed from the side from the same angle. To measure leaf petiole positioning, the angle formed between the hypocotyl and the petiole was measured using the ImageJ software and 90° was subtracted to obtain an angle of petioles relative to horizontal. Both petioles of each plant were measured, and the plant sample size was used to calculate the variance. In Statistical tests, a Student T-test with two-tailed distribution and two-sample unequal variance was used.

Stomatal aperture experiments

Fully expanded rosette leaves were harvested from 4-week-old plants in the dark. The leaves were blended in a Waring blender (Waring Commercial) for 15 sec in 35 ml of distilled water. The epidermal tissues were collected on a 58-µm nylon mesh and rinsed with distilled water. The epidermal fragments were kept in 2ml of basal reaction mixture (5 mM MES / bistrispropane (BTP), 50 mM KCl, and 0.1 mM CaCl2, pH 6.5) and were irradiated with RL at 50 µmol .m^{-2} s^{-1} and superimposed with BL at 10 µmol m^{-2} s^{-1}, for 3 hrs at room temperature. Stomatal apertures were measured in the abaxial epidermis by focusing on the inner lips of stomata. The abaxial epidermises were easily distinguished from the adaxial ones by the shape of their epidermal cells. In each line, the apertures of 45 stomata were determined. All measurements were done between 8:00 am and 11:00 am.

Stomatal conductance experiments

Plants were grown in climate cabinets for 8 to 10 weeks, with a day / night cycle of 8 / 16 hrs, the temperature cycling between 22 / 16 °C and illuminated with WL fluorescent tubes (Osram L36W/25, Munich, Germany) at a photon flux density of 200 µmol m^{-2} s^{-1}. Relative humidity was not controlled. Plants were transferred to the laboratory the night

before measurements, on the next morning (8.00 am), a leaf was excised, its petiole was cut again under water to avoid embolism and kept in water thereafter. A section of the leaf was enclosed in a sandwich-type cuvette (diameter 2.1 cm) with glass windows on the upper and lower side. The abaxial side of the leaf was directed upwards and exposed to a gas stream of 0.5 liter min^{-1}. The relative humidity of the air was 46 %, the temperature was 24°C and the CO_2 concentration was 350 µl l^{-1}. Light was provided by halogen lamps (HLX 64657, Osram, Munich, Germany) to the adaxial side of the leaf and passed through infra red filers (Calflex C, Balzers, Lichtenstein) in combination with color glass filters; blue short pass $\lambda_{1/2}$ 487 nm (5030, Corning Glass Works, Corning, NY) and red long pass $\lambda_{1/2}$ 630 nm (Schott, Mainz, Germany). The photon flux densities were 25 $\mu mol.m^{-2}.s^{-1}$ for BL and 500 $\mu mol.m^{-2}.s^{-1}$ for RL. Transpiration rates were measured by infrared gas analysis technique (Binos, Heraeus, Hanau, Germany).

Chloroplast movement experiments

Chloroplast movement was assessed photometrically by measuring changes in red light transmittance of leaves through time (Walczak and Gabrys, 1980; Jarillo et al., 2001; DeBlasio et al., 2003; DeBlasio et al., 2005) using a microprocessor controlled system based on the design of (Berg et al., 2006). Plants were grown under 12 hrs light photoperiod and 100 - 120 µmol m^{-2} s^{-1} WL was provided by a mixture of cool-white fluorescent and incandescent bulbs. Temperature was 24°C and humidity was not controlled. When plants reached c.a. 45 days old, one adult leaf per plant was detached, its petiole placed between two wet whatman strips, and a region of the lamina between the midvein and the margin was positioned over a light sensor. Epinastic leaf laminas were gently uncurled by making a small section in the margin. Leaves were covered by a black plastic cover containing built-in red-blue LEDs and were dark-adapted overnight. RL transmittance (measured every 5 mins with a 100 µs pulse) was monitored for one hour in the absence of BL before chloroplast relocalization was triggered by ten increments of BL (0.1 - 120 µmol m^{-2} s^{-1}). BL-induced chloroplast movement was determined by calculating the percentage change in RL transmittance relative to the dark position. Percentage change in red light transmittance (%Δt) was determined as $\%\Delta t = (T_t\text{-}T_D)/I*100$, where T_t was the transmitted red light at time t, T_D was the mean

transmitted red light in dark acclimated leaves (mean value over the first hour of measurement) and *I* was the incident red light. To account for differences in leaf transmittance all data were scaled to have and initial transmittance of 10%.

Growth experiments

Approximately 15 seeds were sown directly on moist soil on aracon pots. After stratification, seeds were incubated in a growth chamber under 70 ± 8 µmol m^{-2} s^{-1} or 150 ± 15 µmol m^{-2} s^{-1} WL under transparent plastic domes. Domes were removed after 36 hours. Trays were shuffled every two days and plants were similarly watered from below. At three different time points between 14 and 31 dai, hypocotyls were sectioned and the green tissue fresh weight of plants was measured using a precision balance.

Determination of epidermal cell size and stomata numbers

Abaxial and adaxial sides of leaves were gently pressed onto a glass slide containing a layer of nail polish. After drying out, peels of nail polish were pulled off using fine forceps and mounted in a drop of water on a glass slide. To maintain the lamina of epinastic mutants flat, the leaves were sectioned at apex and artificially flattened on double adhesive tape. Regions of the lamina analyzed were located between 25 and 75% of the distance between the tip and the base of the leaf and halfway between midrib and margin. Bright field digital photographs were taken from one focal plane view using a plan neofluore 0.3 10× objective (100-fold magnification) on an inverted confocal LSM510 Axiovert 200M Zeiss microscope. Micrographs of nail polish prints and of a micrometric ruler were printed onto paper. Outlines of 40 to 130 cells were drawn then scanned, and the total area was determined by ImageJ software (http://rsb.info.nih.gov/ij/) and the number of epidermal cells and stomata were counted within that area. From these measurements the average cell area (µm^2) and stomatal density (mm^{-1}) were calculated. Five leaves were analyzed and mean ±SD were calculated.

Protein fractionation and immunoprecipitation experiments

Plants were grown on ½ MS agar in a phytotron (100 µmol m^{-2} s^{-1} continuous WL, 22°C) for 15 days (growth stage 1.05). About 300 mg of aerial parts of plants were harvested

and ground in 1 ml of cold extraction buffer EB (300 mM sucrose, 150 mM NaCl, 10 mM K-acetate, 5 mM EDTA, 100 mM AEBSF (prefabloc), 1% of protease inhibitor mixture for plant extracts (Sigma P9599), 50 mM Hepes pH 7.9) using a pestle and mortar. Cell debris were separated (5 mins at 1000*g*, 4°C), the supernatant (T1) was collected, and microsomes were isolated by ultracentrifugation (P1 and S2; 75 mins at 75'000*g*, 4°C). The microsomal pellet (P1) was resuspended in 750 µl of EB plus 0.5% (v/v) Triton X-100 to solubilize membrane-associated proteins. Suspension was centrifuged 5 mins (P2 and S3; 16'000*g*, 4°C) and 60 µl of magnetic beads coupled to monoclonal anti-GFP antibodies (Miletenyi Biotec, Product number 130-091-125) were added to the supernatant (INPUT, S3). The immunoprecipitation solution was gently mixed on a rotating wheel for 1 hr at 4°C and antiGFP-coupled beads were recovered using a magnetic column. After extensive washes (20 column volumes of EB plus 0.5% (v/v) Triton X-100), immunoprecipitated proteins (IP) were collected by adding 50µl of 95°C 2× Laemmli buffer onto the column.

Western blotting

Proteins were separated on 10% SDS/PAGE gels and transferred onto nitrocellulose with 100mM CAPS pH11 + 10% (v/v) methanol. The blots were probed with anti-DET3, anti-NPH3, anti-PKS1 and anti-GFP antisera as described (Lariguet et al., 2006). Polyclonal anti-PKS2 antibodies were raised as follow: a *PKS2* cDNA sequence encoding the first 155 amino acids was fused to the C-terminus of glutathione-S-transferase (GST) coding sequence using the BamH1 site in the pGEX-4T-1 vector (to generate pMC30). GST-PKS2(aa1-155) recombinant proteins were produced in *E. coli* by inducing gene expression with 0.1mM IPTG for 3hrs at 20°C. Purified soluble GST-PKS(aa1-155) proteins were used to immunize rabbits. After six boosts the serum of one rabbit was retrieved and polyclonal antibodies specific to PKS2 were obtained by negative (using protein extracts from *pks2-2* plants) and positive (using purified GST-PKS2(aa1-155) proteins) purifications. Anti-PKS2 antibodies were used at a 1/300 dilution in PBS, 0.1% Tween 20, and 5% nonfat milk.

GUS staining experiments

GUS staining was done based on the protocol of Lagarde et al. (1996) (Lagarde et al., 1996). Briefly, plant tissues were prefixed for 45 mins at room temperature in prefixing solution [0.5% (v/v) formaldehyde; 0.05% Triton X-100; 50mM NaPO4 pH7], rinsed in 50mM NaPO4 ph7 and incubated at 37°C in solution containing coloration substrate [0.5mM K-ferricyanide; 0.5mM K-ferrocyanide; 0.05% (v/v) Triton X-100; 1mM X-Gluc; 50mM NaPO4 pH7]. Duration of coloration was 24 hours. Tissues were then fixed in 2% (v/v) formaldehyde + 0.5% (v/v) glutaraldehyde + 100mM NaPO4 pH7 for 3 hours at 4°C and rinsed with 100mM NaPO4 pH7. Green tissues were clarified using a series of ethanol concentration (10-70% (v/v)). Pictures of samples were obtained using a flatbed scanner. Three independent *PKS2:GUS* lines were analyzed (Lariguet et al. 2003) and gave similar expression patterns. The result for one representative sample is shown. One *DR5:GUS* line was analyzed (Ulmasov et al., 1997).

Protoplast auxin efflux experiments

Intact Arabidopsis mesophyll protoplasts were prepared from rosette leaves of plants grown on soil under white light (100 µmol m^{-2} s^{-1}, 8 h light/16 h dark, 21°C) and auxin efflux experiments were performed as described in (Geisler et al., 2005). In short, intact protoplasts were isolated as described, and loaded by incubation with 1µl/ml ^{3}H-IAA (specific activity 20 Ci/mmol, American Radiolabeled Chemicals, St. Louis, MO) on ice. Retained radioactivity was determined by scintillation counting of protoplasts separated by percoll gradient centrifugation, and relative import of initial loading (loading prior to incubation) is calculated as follows: (radioactivity in the protoplasts at time t) - (radioactivity in the protoplasts at time t = 0))*(100%)/(radioactivity in the protoplasts at t=0).

Acknowledgements

We thank Martine Trevisan, Laure Allenbach and Vincent Vincenzetti for technical assistance; Emmanuel Liscum and Karin Schumacher for NPH3 and DET3 antibodies respectively; Akira Nagatani for providing the PHOT2::PHOT2-GFP line and Winslow Briggs for providing the PHOT1:PHOT1-GFP line.

Literature cited:

Autran D, Jonak C, Belcram K, Beemster GT, Kronenberger J, Grandjean O, Inze D, Traas J (2002) Cell numbers and leaf development in Arabidopsis: a functional analysis of the STRUWWELPETER gene. Embo J **21:** 6036-6049

Bainbridge K, Guyomarc'h S, Bayer E, Swarup R, Bennett M, Mandel T, Kuhlemeier C (2008) Auxin influx carriers stabilize phyllotactic patterning. Genes Dev **22:** 810-823

Berg R, Koniger M, Schjeide BM, Dikmak G, Kohler S, Harris GC (2006) A simple low-cost microcontroller-based photometric instrument for monitoring chloroplast movement. Photosynth Res **87:** 303-311

Blakeslee JJ, Bandyopadhyay A, Peer WA, Makam SN, Murphy AS (2004) Relocalization of the PIN1 auxin efflux facilitator plays a role in phototropic responses. Plant Physiol **134:** 28-31

Boccalandro HE, De Simone SN, Bergmann-Honsberger A, Schepens I, Fankhauser C, Casal JJ (2008) PHYTOCHROME KINASE SUBSTRATE1 regulates root phototropism and gravitropism. Plant Physiol **146:** 108-115

Bogre L, Okresz L, Henriques R, Anthony RG (2003) Growth signalling pathways in Arabidopsis and the AGC protein kinases. Trends Plant Sci **8:** 424-431

Boyes DC, Zayed AM, Ascenzi R, McCaskill AJ, Hoffman NE, Davis KR, Gorlach J (2001) Growth stage-based phenotypic analysis of Arabidopsis: a model for high throughput functional genomics in plants. Plant Cell **13:** 1499-1510

Braun N, Wyrzykowska J, Muller P, David K, Couch D, Perrot-Rechenmann C, Fleming AJ (2008) Conditional Repression of AUXIN BINDING PROTEIN1 Reveals That It Coordinates Cell Division and Cell Expansion during Postembryonic Shoot Development in Arabidopsis and Tobacco. Plant Cell

Briggs WR, Christie JM (2002) Phototropins 1 and 2: versatile plant blue-light receptors. Trends Plant Sci **7:** 204-210

Casal JJ (2000) Phytochromes, cryptochromes, phototropin: photoreceptor interactions in plants. Photochem Photobiol **71:** 1-11

Celaya RB, Liscum E (2005) Phototropins and associated signaling: providing the power of movement in higher plants. Photochem Photobiol **81:** 73-80

Chen M, Chory J, Fankhauser C (2004) Light signal transduction in higher plants. Annu Rev Genet **38:** 87-117

Cheng Y, Qin G, Dai X, Zhao Y (2007) NPY1, a BTB-NPH3-like protein, plays a critical role in auxin-regulated organogenesis in Arabidopsis. Proc Natl Acad Sci U S A **104:** 18825-18829

Cheng Y, Qin G, Dai X, Zhao Y (2008) NPY genes and AGC kinases define two key steps in auxin-mediated organogenesis in Arabidopsis. Proc Natl Acad Sci U S A **105:** 21017-21022

Christie JM (2007) Phototropin Blue-Light Receptors. Annu Rev Plant Biol

Cutler SR, Ehrhardt DW, Griffitts JS, Somerville CR (2000) Random GFP::cDNA fusions enable visualization of subcellular structures in cells of Arabidopsis at a high frequency. Proc Natl Acad Sci U S A **97:** 3718-3723

DeBlasio SL, Luesse DL, Hangarter RP (2005) A plant-specific protein essential for blue-light-induced chloroplast movements. Plant Physiol **139:** 101-114

DeBlasio SL, Mullen JL, Luesse DR, Hangarter RP (2003) Phytochrome modulation of blue light-induced chloroplast movements in Arabidopsis. Plant Physiol **133:** 1471-1479

Demarsy E, Fankhauser C (2009) Higher plants use LOV to perceive blue light. Curr Opin Plant Biol

Doi M, Shigenaga A, Emi T, Kinoshita T, Shimazaki K (2004) A transgene encoding a blue-light receptor, phot1, restores blue-light responses in the Arabidopsis phot1 phot2 double mutant. J Exp Bot **55:** 517-523

Donnelly PM, Bonetta D, Tsukaya H, Dengler RE, Dengler NG (1999) Cell cycling and cell enlargement in developing leaves of Arabidopsis. Dev Biol **215:** 407-419

Duarte JM, Cui L, Wall PK, Zhang Q, Zhang X, Leebens-Mack J, Ma H, Altman N, dePamphilis CW (2006) Expression pattern shifts following duplication indicative of subfunctionalization and neofunctionalization in regulatory genes of Arabidopsis. Mol Biol Evol **23:** 469-478

Esmon CA, Tinsley AG, Ljung K, Sandberg G, Hearne LB, Liscum E (2006) A gradient of auxin and auxin-dependent transcription precedes tropic growth responses. Proc Natl Acad Sci U S A **103:** 236-241

Fankhauser C, Yeh KC, Lagarias JC, Zhang H, Elich TD, Chory J (1999) PKS1, a substrate phosphorylated by phytochrome that modulates light signaling in Arabidopsis. Science **284:** 1539-1541

Franklin KA, Whitelam GC (2004) Light signals, phytochromes and cross-talk with other environmental cues. J Exp Bot **55:** 271-276

Franklin KA, Whitelam GC (2005) Phytochromes and shade-avoidance responses in plants. Ann Bot (Lond) **96:** 169-175

Friml J, Wisniewska J, Benkova E, Mendgen K, Palme K (2002) Lateral relocation of auxin efflux regulator PIN3 mediates tropism in Arabidopsis. Nature **415:** 806-809

Furutani M, Kajiwara T, Kato T, Treml BS, Stockum C, Torres-Ruiz RA, Tasaka M (2007) The gene MACCHI-BOU 4/ENHANCER OF PINOID encodes a NPH3-like protein and reveals similarities between organogenesis and phototropism at the molecular level. Development

Galen C, Rabenold JJ, Liscum E (2007) Functional ecology of a blue light photoreceptor: effects of phototropin-1 on root growth enhance drought tolerance in Arabidopsis thaliana. New Phytol **173:** 91-99

Geisler M, Blakeslee JJ, Bouchard R, Lee OR, Vincenzetti V, Bandyopadhyay A, Titapiwatanakun B, Peer WA, Bailly A, Richards EL, Ejendal KF, Smith AP, Baroux C, Grossniklaus U, Muller A, Hrycyna CA, Dudler R, Murphy AS, Martinoia E (2005) Cellular efflux of auxin catalyzed by the Arabidopsis MDR/PGP transporter AtPGP1. Plant J **44:** 179-194

Haga K, Takano M, Neumann R, Iino M (2005) The Rice COLEOPTILE PHOTOTROPISM1 gene encoding an ortholog of Arabidopsis NPH3 is required for phototropism of coleoptiles and lateral translocation of auxin. Plant Cell **17:** 103-115

Holland JJ, Roberts D, Liscum E (2009) Understanding phototropism: from Darwin to today. J Exp Bot

Huala E, Oeller PW, Liscum E, Han IS, Larsen E, Briggs WR (1997) Arabidopsis NPH1: a protein kinase with a putative redox-sensing domain. Science **278:** 2120-2123

Iino M (2006) Toward understanding the ecological functions of tropisms: interactions among and effects of light on tropisms. Curr Opin Plant Biol **9:** 89-93

Inada S, Ohgishi M, Mayama T, Okada K, Sakai T (2004) RPT2 is a signal transducer involved in phototropic response and stomatal opening by association with phototropin 1 in Arabidopsis thaliana. Plant Cell **16:** 887-896

Inoue S, Kinoshita T, Matsumoto M, Nakayama KI, Doi M, Shimazaki K (2008b) Blue light-induced autophosphorylation of phototropin is a primary step for signaling. Proc Natl Acad Sci U S A **105:** 5626-5631

Inoue S-I, Kinoshita T, Takemiya A, Doi M, Shimazaki K-I (2008a) Leaf Positioning of Arabidopsis in Response to Blue Light. Molecular Plant **1:** 15-26

Inoue Y, Shibata K (1973) Light-induced chloroplast rearrangements and their action spectra as measured by absorption spectrophotometry. Planta **114:** 341-358

Jarillo JA, Gabrys H, Capel J, Alonso JM, Ecker JR, Cashmore AR (2001) Phototropin-related NPL1 controls chloroplast relocation induced by blue light. Nature **410:** 952-954

Jiao Y, Lau OS, Deng XW (2007) Light-regulated transcriptional networks in higher plants. Nat Rev Genet **8:** 217-230

Kagawa T, Sakai T, Suetsugu N, Oikawa K, Ishiguro S, Kato T, Tabata S, Okada K, Wada M (2001) Arabidopsis NPL1: a phototropin homolog controlling the chloroplast high-light avoidance response. Science **291:** 2138-2141

Kasahara M, Kagawa T, Oikawa K, Suetsugu N, Miyao M, Wada M (2002) Chloroplast avoidance movement reduces photodamage in plants. Nature **420:** 829-832

Keller CP, Van Volkenburgh E (1997) Auxin-Induced Epinasty of Tobacco Leaf Tissues (A Nonethylene-Mediated Response). Plant Physiol **113:** 603-610

Kerstetter RA, Poethig RS (1998) The specification of leaf identity during shoot development. Annu Rev Cell Dev Biol **14:** 373-398

Khanna R, Shen Y, Toledo-Ortiz G, Kikis EA, Johannesson H, Hwang YS, Quail PH (2006) Functional profiling reveals that only a small number of phytochrome-regulated early-response genes in Arabidopsis are necessary for optimal deetiolation. Plant Cell **18:** 2157-2171

Kinoshita T, Doi M, Suetsugu N, Kagawa T, Wada M, Shimazaki K (2001) Phot1 and phot2 mediate blue light regulation of stomatal opening. Nature **414:** 656-660

Kong SG, Suzuki T, Tamura K, Mochizuki N, Hara-Nishimura I, Nagatani A (2006) Blue light-induced association of phototropin 2 with the Golgi apparatus. Plant J **45:** 994-1005

Lagarde D, Basset M, Lepetit M, Conejero G, Gaymard F, Astruc S, Grignon C (1996) Tissue-specific expression of Arabidopsis AKT1 gene is consistent with a role in K+ nutrition. Plant J **9:** 195-203

Lariguet P, Boccalandro HE, Alonso JM, Ecker JR, Chory J, Casal JJ, Fankhauser C (2003) A growth regulatory loop that provides homeostasis to phytochrome a signaling. Plant Cell **15:** 2966-2978

Lariguet P, Fankhauser C (2004) Hypocotyl growth orientation in blue light is determined by phytochrome A inhibition of gravitropism and phototropin promotion of phototropism. Plant J **40:** 826-834

Lariguet P, Schepens I, Hodgson D, Pedmale UV, Trevisan M, Kami C, de Carbonnel M, Alonso JM, Ecker JR, Liscum E, Fankhauser C (2006) PHYTOCHROME KINASE SUBSTRATE 1 is a phototropin 1 binding protein required for phototropism. Proc Natl Acad Sci U S A **103:** 10134-10139

Li L-C, Kang D-M, Chen Z-L, Qu L-J (2007) Hormonal Regulation of Leaf Morphogenesis in *Arabidopsis*. Journal of Intergrative Plant Biology **49:** 75-80

Liscum E, Briggs WR (1995) Mutations in the NPH1 locus of Arabidopsis disrupt the perception of phototropic stimuli. Plant Cell **7:** 473-485

Michniewicz M, Zago MK, Abas L, Weijers D, Schweighofer A, Meskiene I, Heisler MG, Ohno C, Zhang J, Huang F, Schwab R, Weigel D, Meyerowitz EM, Luschnig C, Offringa R, Friml J (2007) Antagonistic regulation of PIN phosphorylation by PP2A and PINOID directs auxin flux. Cell **130:** 1044-1056

Millenaar FF, van Zanten M, Cox MC, Pierik R, Voesenek LA, Peeters AJ (2009) Differential petiole growth in Arabidopsis thaliana: photocontrol and hormonal regulation. New Phytol **184:** 141-152

Molas ML, Kiss JZ (2008) PKS1 plays a role in red-light-based positive phototropism in roots. Plant Cell Environ **31:** 842-849

Motchoulski A, Liscum E (1999) Arabidopsis NPH3: A NPH1 photoreceptor-interacting protein essential for phototropism. Science **286:** 961-964

Mullen JL, Weinig C, Hangarter RP (2006) Shade avoidance and the regulation of leaf inclination in *Arabidopsis.* Plant Cell Environ **29:** 1099-1106

Nagashima A, Suzuki G, Uehara Y, Saji K, Furukawa T, Koshiba T, Sekimoto M, Fujioka S, Kuroha T, Kojima M, Sakakibara H, Fujisawa N, Okada K, Sakai T (2008) Phytochromes and cryptochromes regulate the differential growth of Arabidopsis hypocotyls in both a PGP19-dependent and a PGP19-independent manner. Plant J

Neff MM, Fankhauser C, Chory J (2000) Light: an indicator of time and place. Genes Dev **14:** 257-271

Noh B, Bandyopadhyay A, Peer WA, Spalding EP, Murphy AS (2003) Enhanced gravi- and phototropism in plant mdr mutants mislocalizing the auxin efflux protein PIN1. Nature **423:** 999-1002

Oppenheimer DG, Herman PL, Sivakumaran S, Esch J, Marks MD (1991) A myb gene required for leaf trichome differentiation in Arabidopsis is expressed in stipules. Cell **67:** 483-493

Pedmale UV, Liscum E (2007) Regulation of phototropic signaling in Arabidopsis via phosphorylation state changes in the phototropin 1-interacting protein NPH3. J Biol Chem **282:** 19992-20001

Poethig RS (1997) Leaf morphogenesis in flowering plants. Plant Cell **9:** 1077-1087

Robert HS, Offringa R (2008) Regulation of auxin transport polarity by AGC kinases. Curr Opin Plant Biol **11:** 495-502

Roelfsema MR, Hanstein S, Felle HH, Hedrich R (2002) CO2 provides an intermediate link in the red light response of guard cells. Plant J **32:** 65-75

Roelfsema MR, Hedrich R (2005) In the light of stomatal opening: new insights into 'the Watergate'. New Phytol **167:** 665-691

Roman G, Lubarsky B, Kieber JJ, Rothenberg M, Ecker JR (1995) Genetic analysis of ethylene signal transduction in Arabidopsis thaliana: five novel mutant loci integrated into a stress response pathway. Genetics **139:** 1393-1409

Sakai T, Kagawa T, Kasahara M, Swartz TE, Christie JM, Briggs WR, Wada M, Okada K (2001) Arabidopsis nph1 and npl1: blue light receptors that mediate both phototropism and chloroplast relocation. Proc Natl Acad Sci U S A **98:** 6969-6974

Sakamoto K, Briggs WR (2002) Cellular and subcellular localization of phototropin 1. Plant Cell **14:** 1723-1735

Savaldi-Goldstein S, Chory J (2008) Growth coordination and the shoot epidermis. Curr Opin Plant Biol **11:** 42-48

Schepens I, Boccalandro HE, Kami C, Casal JJ, Fankhauser C (2008) PHYTOCHROME KINASE SUBSTRATE4 Modulates Phytochrome-Mediated Control of Hypocotyl Growth Orientation. Plant Physiol **147:** 661-671

Shimazaki K, Doi M, Assmann SM, Kinoshita T (2007) Light regulation of stomatal movement. Annu Rev Plant Biol **58:** 219-247

Stone BB, Stowe-Evans EL, Harper RM, Brandon Celaya R, Ljung K, Sandberg G, Liscum E (2008) Disruptions in AUX1-Dependent Auxin Influx Alter Hypocotyl Phototropism in Arabidopsis. Molecular Plant **1:** 129-144

Sullivan S, Thomson CE, Kaiserli E, Christie JM (2009) Interaction specificity of Arabidopsis 14-3-3 proteins with phototropin receptor kinases. FEBS Lett **583:** 2187-2193

Sullivan S, Thomson CE, Lamont DJ, Jones MA, Christie JM (2008) In Vivo Phosphorylation Site Mapping and Functional Characterization of Arabidopsis Phototropin 1. Molecular Plant **1:** 178-194

Takemiya A, Inoue S, Doi M, Kinoshita T, Shimazaki K (2005) Phototropins promote plant growth in response to blue light in low light environments. Plant Cell **17:** 1120-1127

Tao Y, Ferrer JL, Ljung K, Pojer F, Hong F, Long JA, Li L, Moreno JE, Bowman ME, Ivans LJ, Cheng Y, Lim J, Zhao Y, Ballare CL, Sandberg G, Noel JP, Chory J (2008) Rapid synthesis of auxin via a new tryptophan-dependent pathway is required for shade avoidance in plants. Cell **133:** 164-176

Tatematsu K, Kumagai S, Muto H, Sato A, Watahiki MK, Harper RM, Liscum E, Yamamoto KT (2004) MASSUGU2 encodes Aux/IAA19, an auxin-regulated protein that functions together with the transcriptional activator NPH4/ARF7 to regulate differential growth responses of hypocotyl and formation of lateral roots in Arabidopsis thaliana. Plant Cell **16:** 379-393

Tokutomi S, Matsuoka D, Zikihara K (2008) Molecular structure and regulation of phototropin kinase by blue light. Biochim Biophys Acta **1784:** 133-142

Trojan A, Gabrys H (1996) Chloroplast Distribution in Arabidopsis thaliana (L.) Depends on Light Conditions during Growth. Plant Physiol **111:** 419-425

Ulmasov T, Murfett J, Hagen G, Guilfoyle TJ (1997) Aux/IAA proteins repress expression of reporter genes containing natural and highly active synthetic auxin response elements. Plant Cell **9:** 1963-1971

Walczak T, Gabrys H (1980) New type of photometer for measurements of transmission changes corresponding to chloroplast movements in leaves. Photosynthetica **14:** 65-72

Whippo CW, Hangarter RP (2006) Phototropism: bending towards enlightenment. Plant Cell **18:** 1110-1119

Figure Legends

Figure 1. *PKS1/PKS2/PKS4* regulate leaf flattening and act in the phot2 pathway. A, Plants were grown for 25 days under 80 ± 8 μmol m^{-2} s^{-1} white light (WL) with a 16 hours light photoperiod at 20°C (until wild type (WT) reached growth stage 1.11; Boyes et al., 2001). The flattening index of leaf number five was calculated by dividing the projection area of intact curled leaves (inset - left) with that of manually uncurled leaves (inset - right). The graph shows average values ± 95% confidence intervals for 17 or 18 plants. Lower pictures of leaf sections illustrate leaf curling. B, Positions of PKS1/2 and NPH3 based on the interpretation of epistasis data.

Figure 2. *PKS2* regulates leaf positioning. Leaf positioning was determined after light treatments by measuring the hypocotyl - petiole angle. 90° was substracted to provide an indication of petiole position relative to horizontal (top right inset in panel A). Light blue histogram bars correspond to 50 μmol m^{-2} s^{-1} RL plus 0.3 μmol m^{-2} s^{-1} BL; dark blue bars correspond to RL plus 5.0 μmol m^{-2} s^{-1} BL. A, Leaf positioning in *pks1*, *pks2*, *pks4* mutants and in the triple mutant. B, Leaf positioning in *PKS2* over-expressing plants. Erros bars indicate mean ± 95% confidence intervals for $21<n<31$ (panel A) and $34<n<57$ plants (panel B).

Figure 3. Genetic analysis of *PKS2* and *NPH3* roles within phot1 and phot2 pathways controlling leaf positioning. Plants were grown as described in figure 2. A, Epistasis between *nph3* and *phot* mutants. B, Epistasis between *pks2*, *nph3* and *phot* mutants. Bars indicate mean ± 95% confidence intervals for $32<n<52$ plants (panel A) and $32<n<55$ plants (panel B). C, Visual comparison of selected mutants grown under high BL. Side views of plants illustrate the positioning of petioles and the flatness of laminae of the first pair of true leaves. Upper views further show lamina epinasty and reduction in light capture. D, Positions of *NPH3* and *PKS2* in phot1 and phot2 pathways in both low BL and high BL based on the interpretation of epistasis data.

Figure 4. PKS2, PKS1 and NPH3 are associated with phot1 and phot2 *in vivo*. Solubilized microsomal proteins were obtained from green tissues of 14-day-old plants grown under 100 μmol m^{-2} s^{-1} white light and were subjected to anti-GFP immunoprecipitation using anti-GFP antibodies. The following genotypes were analyzes: wild type (lanes 1), *35S:GFP-LTi6b* (plasma membraneassociated protein, lanes 2), *PHOT2:PHOT2-GFP phot1-5 phot2-2* (lanes 3), *PHOT1:PHOT1-GFP phot1-5* (lanes 4). INPUT: solubilized microsomes used for the IP. IP: immunoprecipitated material. DET3 serves as a loading control.

Figure 5. *PKS1/PKS2/PKS4* are not required for BL-induced chloroplast relocation or stomatal opening. A, Chloroplast movements in *pks1pks2pks4* mutants. Plants were grown for six weeks under 100-120 μmol m^{-2} s^{-1} WL at 24°C with a 12 hrs photoperiod. Leaves were dark-adapted for 18 hours and then exposed to a progressive increase of BL fluence rate from 0.1 to 120 μmol m^{-2} s^{-1}. Plots show dose response curves corresponding to the change (in percent) of RL transmittance of leaves relative to the average transmittance measured in darktreated leaves. Data points show average ± SD of $9<n<13$ plants. B, Isolated epidermal peels were obtained from rosette leaves of 4-week-old plants and irradiated for 3 hrs at 24°C under red light (60 μmol m^{-2} s^{-1} RL) or red light (50 μmol.m-2.s-1) plus blue light (10 μmol m^{-2} s^{-1}, RL + BL). The average aperture of 45 stomata was calculated per experiment. The graph shows average ± SD of three separate experiments.

Figure 6. Growth of wild type and epinastic mutant plants under intermediate white light fluence rates. Plants were grown at 20.5 ± 1°C under 150 ± 15 μmol m^{-2} s^{-1} WL with a 16 hrs light photoperiod and were shuffled around to even out the effects of varying microenvironments. Fresh weight (FW) of green tissues was measured at 14 (A), 19 (B) and 24 (C) days after incubation (dai). Graphs show average values ± 95% confidence intervals for $20<n<36$ plants. Lower pictures show one representative plant for each genotype. Scale bar = 1cm.

Figure 7. Morphological and physiological parameters of wild type and epinastic mutant leaves. A-B, Morphological parameters of leaf number 5 of plants shown in Figure 6C. Light interception area of curled leaves and total leaf area were calculated as in Figure 1. C, Light-induced transpiration in whole leaves. Plants were grown for 8-10 weeks under 200 µmol m^{-2} s^{-1} WL with an 8 hrs light (22°C) / 16 hrs dark (16°C) cycle. After overnight dark-adaptation, the adaxial side of mature leaves was exposed to 500 µmol m^{-2} s^{-1} RL (black bar) for 60 mins and then 25 µmol.m-2.s-1 BL (white bar) was superimposed for 60 mins. Transpiration on the leaf abaxial side was measured over time by infrared gas analysis technique. Graphs show average transpiration levels 10 mins before and 0-35 mins after switching on blue light for 5<n<9 plants (± SE). D, Stomatal density of abaxial epidermis. Prints were obtained from similar leaves than in Figure 1. Average stomatal density was calculated by counting the number of stomata within a measured area comprising 60-120 epidermal pavement cells. Plots show mean ± SD of 5 leave. Different leaf regions were analyzed (margin to midvein, apex to base).

Figure 8. PKS2 may control leaf flattening and positioning by acting on auxin transport regulation. A, Leaf positioning in *PKS2* over-expressing plants under RL. Bars indicate mean ± 95% confidence intervals for 34<n<57 plants. B, Expression pattern of *PKS2* reported by *GUS* expression. Plants were grown for two weeks on agar under 100 µmol m^{-2} s^{-1} continuous WL at 22°C and were incubated with X-GLUC substrate for 24 hours at 37°C for coloration. C, Auxin loading in mesophyl protoplast of Col, pks1, pks2, pks1pks2 and aux1 mutants. Data are average +/- SD n=3. asterisks mark "significant different means from wt (t test, $p<0.05$)".

Supplemental figure files

Supplemental Figures S1-S6 including their figure legends accompany this manuscript.

Figure 1

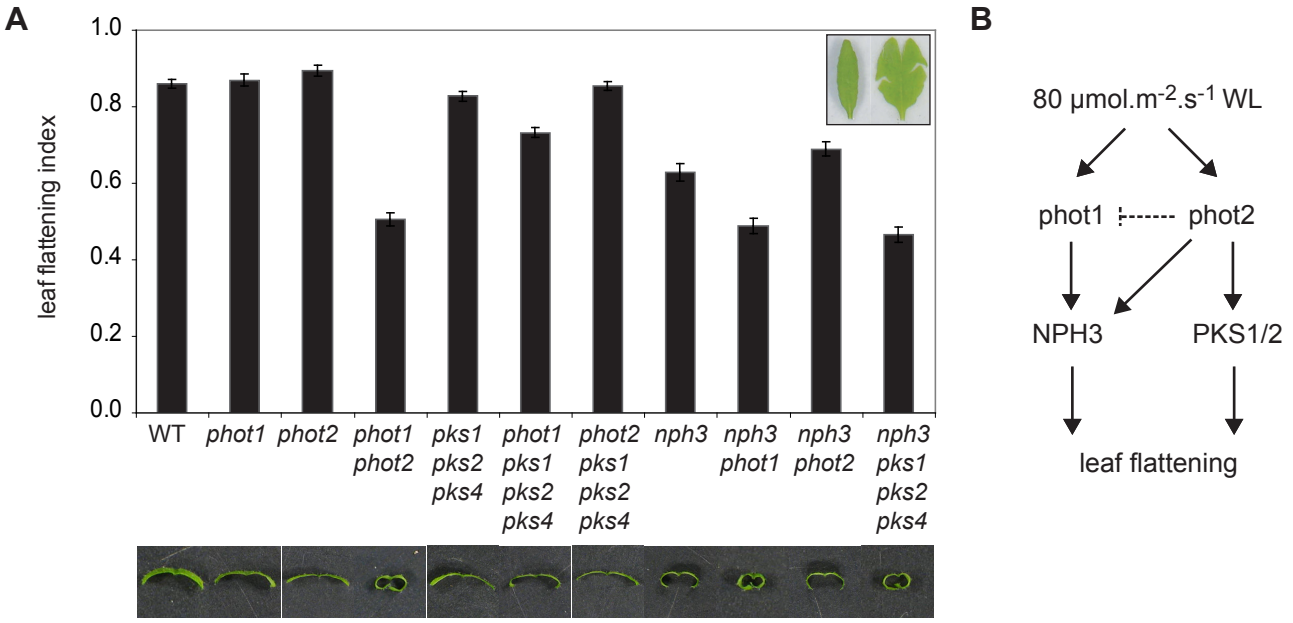

Figure 1. *PKS1/PKS2/PKS4* regulate leaf flattening and act in the phot2 pathway. A, Plants were grown for 25 days under 80 ± 8 µmol.m^{-2}.s^{-1} white light (WL) with a 16 hours light photoperiod at 20°C (until wild type (WT) reached growth stage 1.11; Boyes et al., 2001). The flattening index of leaf number five was calculated by dividing the projection area of intact curled leaves (inset - left) with that of manually uncurled leaves (inset - right). The graph shows average values ± 95% confidence intervals for 17 or 18 plants. Lower pictures of leaf sections illustrate leaf curling. B, Positions of PKS1/2 and NPH3 based on the interpretation of epistasis data.

Figure 2

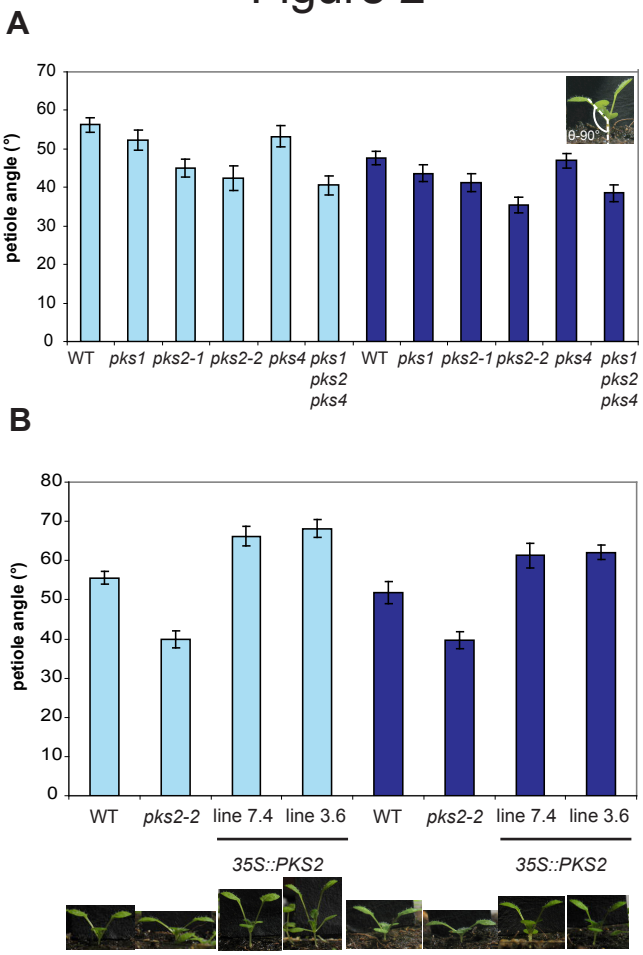

Figure 2. *PKS2* regulates leaf positioning. Leaf positioning was determined after light treatments by measuring the hypocotyl - petiole angle. 90° was substracted to provide an indication of petiole position relative to horizontal (top right inset in panel A). Light blue histogram bars correspond to 50 µmol.m^{-2}.s^{-1} RL plus 0.3 µmol.m^{-2}.s^{-1} BL; dark blue bars correspond to RL plus 5.0 µmol.m^{-2}.s^{-1} BL. A, Leaf positioning in *pks1*, *pks2*, *pks4* mutants and in the triple mutant. B, Leaf positioning in *PKS2* over-expressing plants. Erros bars indicate mean ± 95% confidence intervals for 21<n<31 (panel A) and 34<n<57 plants (panel B).

Figure 3

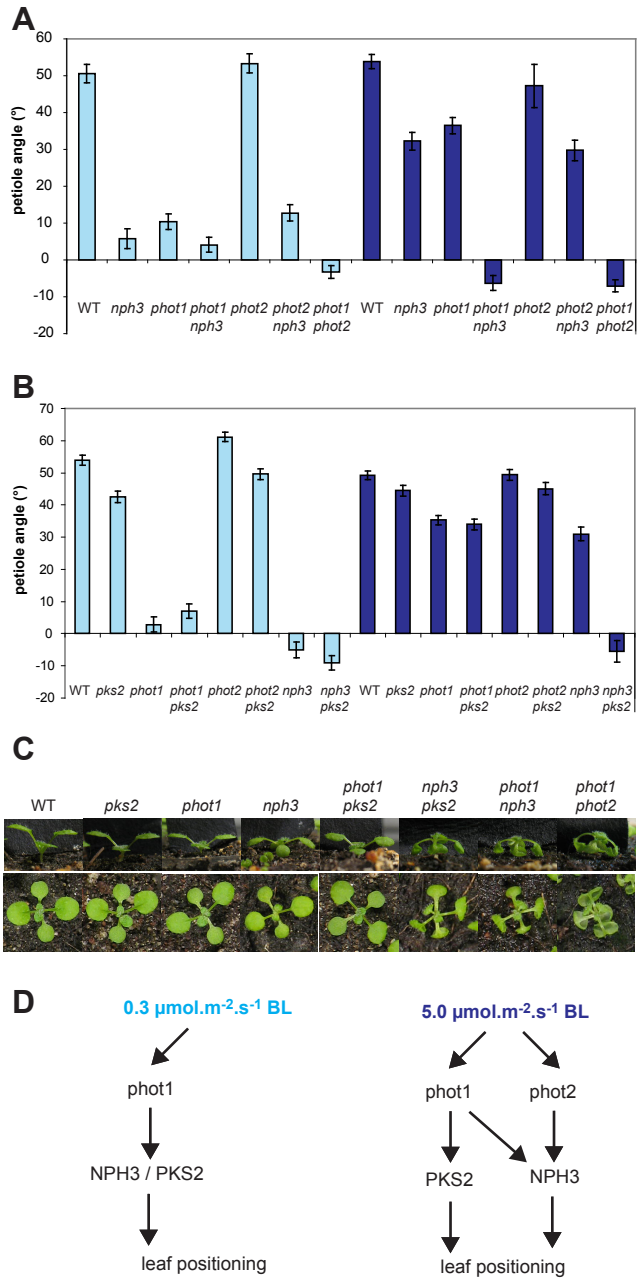

Figure 3. Genetic analysis of *PKS2* and *NPH3* roles within phot1 and phot2 pathways controlling leaf positioning. A, Epistasis between *nph3* and *phot* mutants. B, Epistasis between *pks2*, *nph3* and *phot* mutants. Bars indicate mean ± 95% confidence intervals for 32<n<52 plants (panel A) and 32<n<55 plants (panel B). C, Visual comparison of selected mutants grown under high BL. Side views of plants illustrate the positioning of petioles and the flatness of laminae of the first pair of true leaves. Upper views further show lamina epinasty and reduction in light capture. D, Positions of *NPH3* and *PKS2* in phot1 and phot2 pathways in both low BL and high BL based on the interpretation of epistasis data.

Figure 4

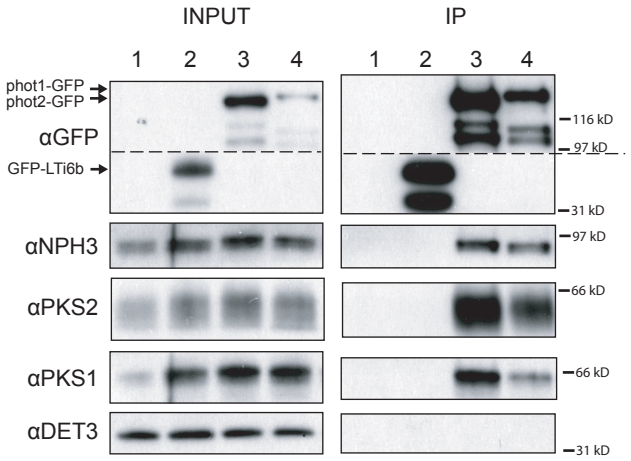

Figure 4. PKS2, PKS1 and NPH3 are associated with phot1 and phot2 *in vivo*. Solubilized microsomal proteins were obtained from green tissues of 14-day-old plants grown under 100 µmol.m^{-2}.s^{-1} white light and were subjected to anti-GFP immunoprecipitation using anti-GFP antibodies. The following genotypes were analyzes: wild type (lanes 1), *35S:GFP-LTi6b* (plasma membrane-associated protein, lanes 2), *PHOT2:PHOT2-GFP phot1-5phot2-2* (lanes 3), *PHOT1:PHOT1-GFP phot1-5* (lanes 4). INPUT: solubilized microsomes used for the IP. IP: immunoprecipitated material. DET3 serves as a loading control.

Figure 5

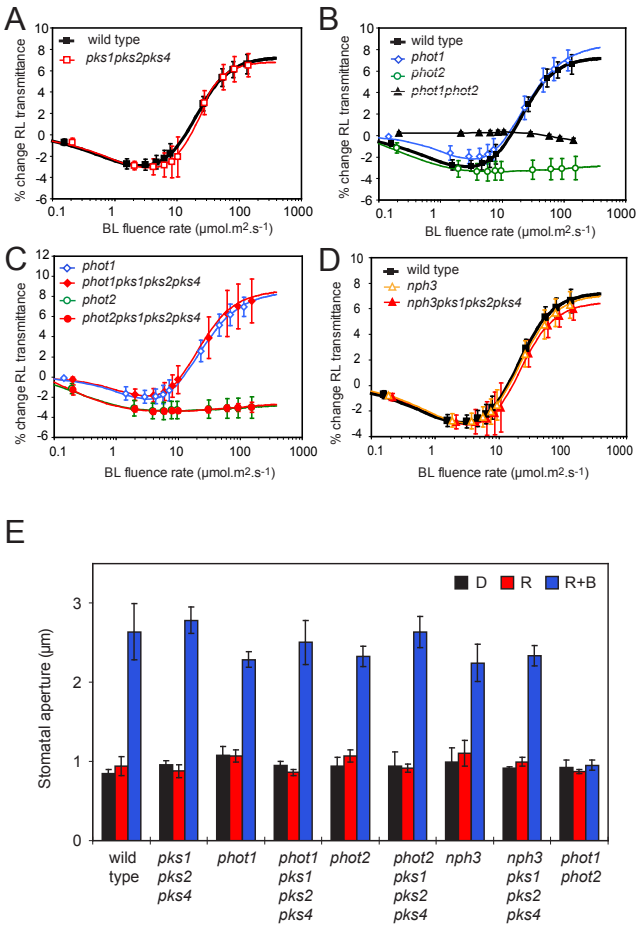

Figure 5. *PKS1/PKS2/PKS4* are not required for BL-induced chloroplast relocation or stomatal opening.
A, Chloroplast movements in *pks1pks2pks4* mutants. Plants were grown for six weeks under 100-120 µmol.m^{-2}.s^{-1} WL at 24°C with a 12 hrs photoperiod. Leaves were dark-adapted for 18 hours and then exposed to a progressive increase of BL fluence rate from 0.1 to 120 µmol.m^{-2}.s^{-1}. Plots show dose response curves corresponding to the change (in percent) of RL transmittance of leaves relative to the average transmittance measured in dark-treated leaves. Data points show average ± SD of 9<n<13 plants. B, Isolated epidermal peels were obtained from rosette leaves of 4-week-old plants and irradiated for 3 hrs at 24°C under red light (60 µmol.m^{-2}.s^{-1} RL) or red light (50 µmol.m^{-2}.s^{-1}) plus blue light (10 µmol.m^{-2}.s^{-1}, RL + BL). The average aperture of 45 stomata was calculated per experiment. The graph shows average ± SD of three separate experiments.

Figure 6

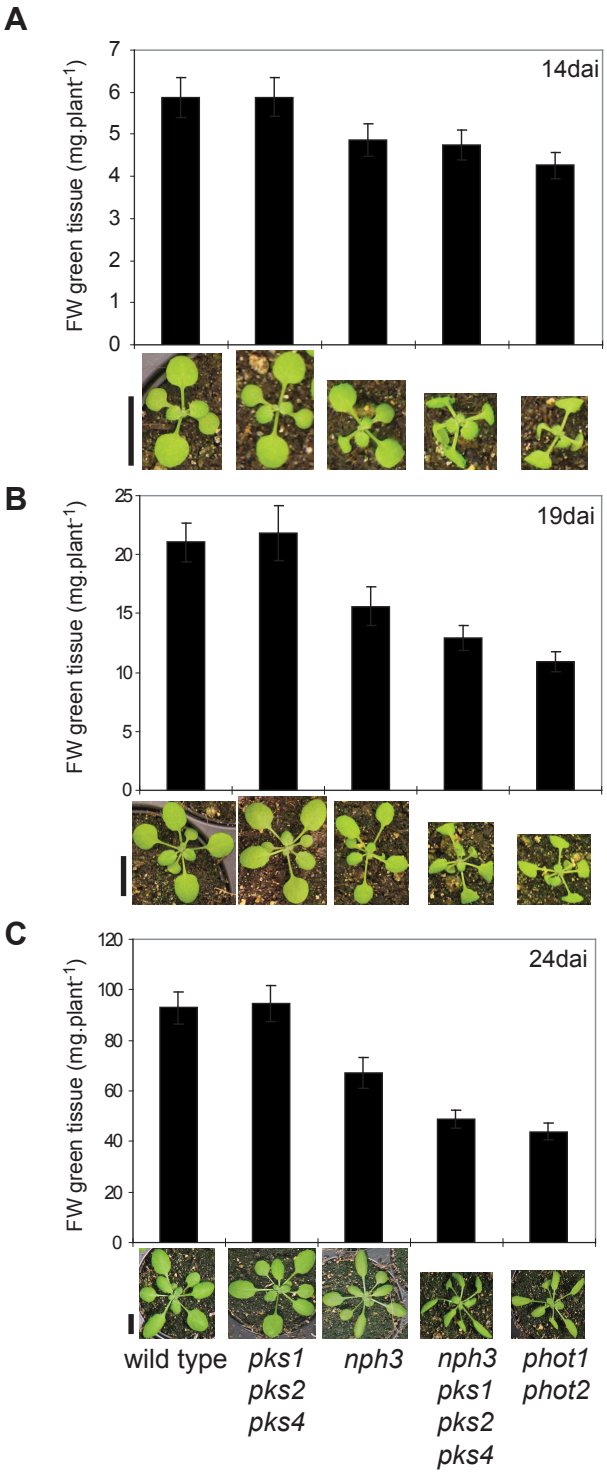

Figure 6. Growth of wild type and epinastic mutant plants under intermediate white light fluence rates. Plants were grown at 20.5 ± 1°C under 150 ± 15 µmol.m^{-2}.s^{-1} WL with a 16 hrs light photoperiod and were shuffled around to even out the effects of varying microenvironments. Fresh weight (FW) of green tissues was measured at 14 (A), 19 (B) and 24 (C) days after incubation (dai). Graphs show average values ± 95% confidence intervals for 20<n<36 plants. Lower pictures show one representative plant for each genotype. Scale bar = 1cm.

Figure 7

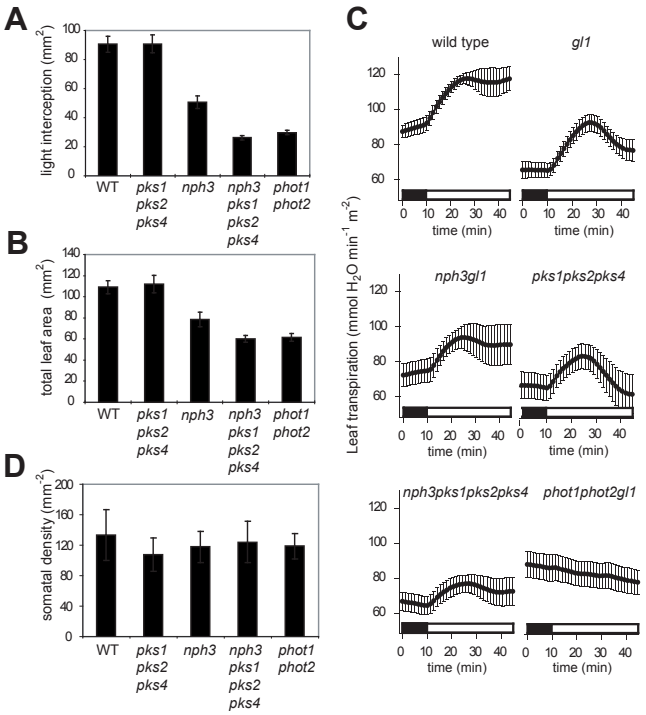

Figure 7. Morphological and physiological parameters of wild type and epinastic mutant leaves. A-B, Morphological parameters of leaf number 5 of plants shown in Figure 6C. Light interception area of curled leaves and total leaf area were calculated as in Figure 1. C, Light-induced transpiration in whole leaves. Plants were grown for 8-10 weeks under 200 $\mu mol.m^{-2}.s^{-1}$ WL with an 8 hrs light (22°C) / 16 hrs dark (16°C) cycle. After overnight dark-adaptation, the adaxial side of mature leaves was exposed to 500 $\mu mol.m^{-2}.s^{-1}$ RL (black bar) for 60 mins and then 25 $\mu mol.m^{-2}.s^{-1}$ BL (white bar) was superimposed for 60 mins. Transpiration on the leaf abaxial side was measured over time by infrared gas analysis technique. Graphs show average transpiration levels 10 mins before and 0-35 mins after switching on blue light for $5<n<9$ plants (± SE). D, Stomatal density of abaxial epidermis. Prints were obtained from similar leaves than in Figure 1. Average stomatal density was calculated by counting the number of stomata within a measured area comprising 60-120 epidermal pavement cells. Plots show mean ± SD of 5 leave. Different leaf regions were analyzed (margin to midvein, apex to base).

Figure 8

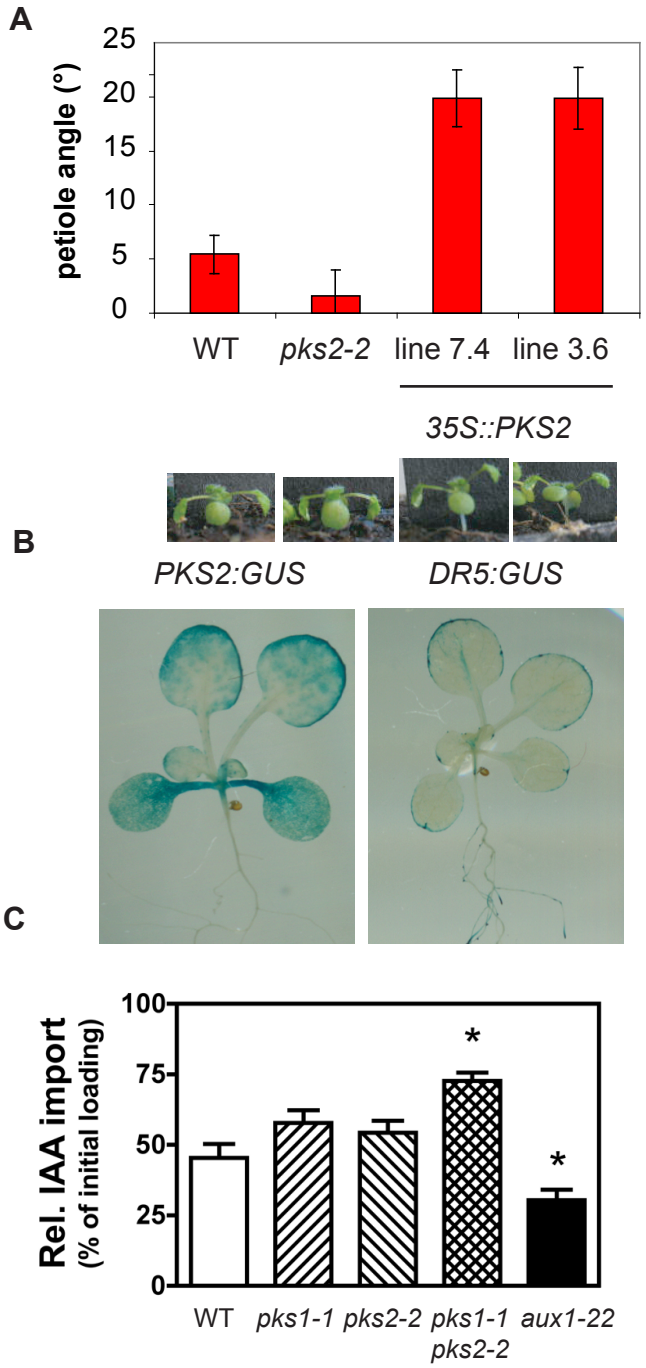

Figure 8. PKS2 may control leaf flattening and positioning by acting on auxin transport regulation. A, Leaf positioning in *PKS2* over-expressing plants under RL. Bars indicate mean ± 95% confidence intervals for 34<n<57 plants. B, Expression pattern of *PKS2* reported by *GUS* expression. Plants were grown for two weeks on agar under 100 µmol.m^{-2}.s^{-1} continuous WL at 22°C and were incubated with X-GLUC substrate for 24 hours at 37°C for coloration. C, Auxin loading in mesophyl protoplast of wild type (WT), *pks1*, *pks2*, *pks1pks2* and *aux1* mutants. Data are average +/- SD n=3. Asterisks mark "significant different means from WT (t test, p<0.05)".

Figure S1

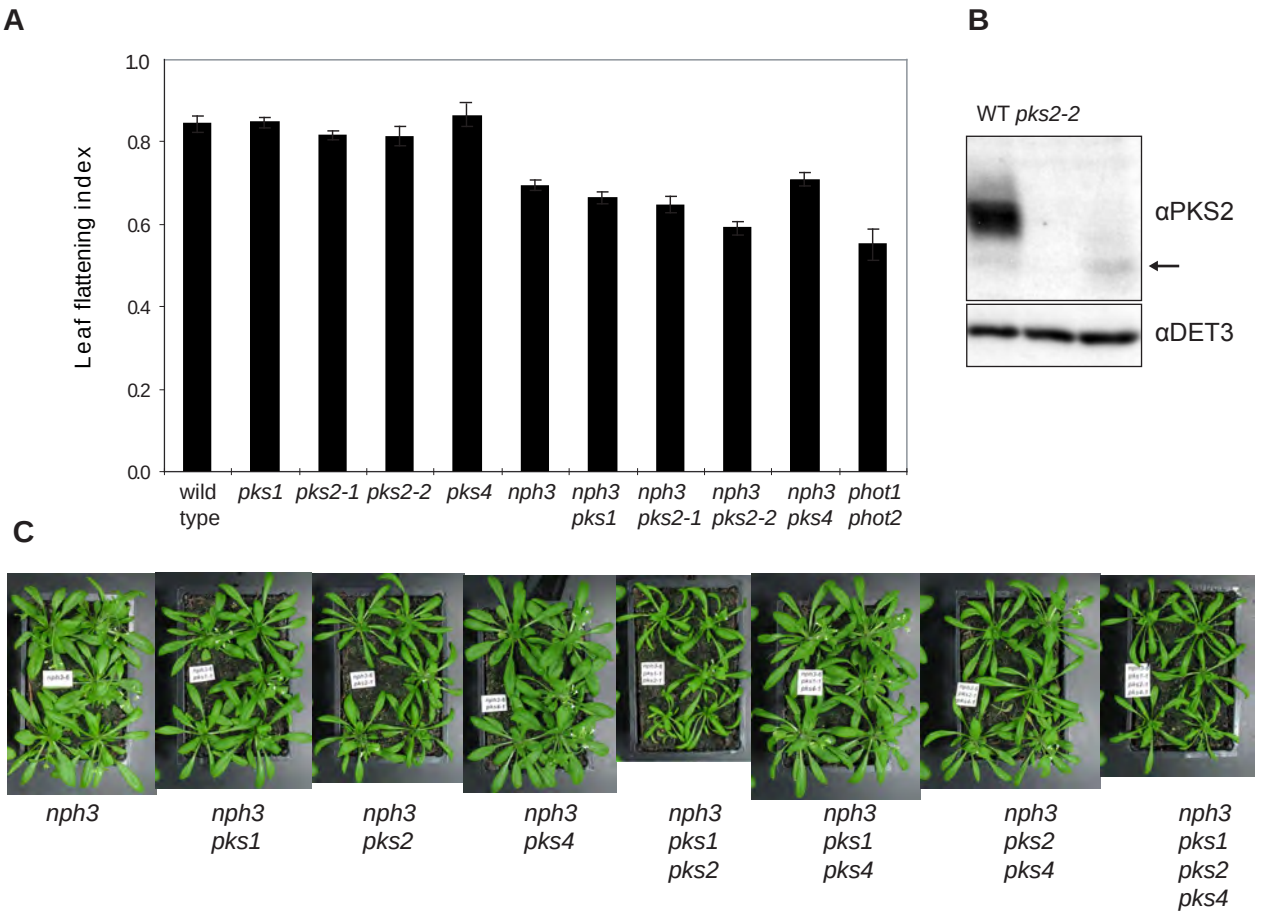

Figure S1. *PKS2* plays a predominant role in leaf flattening. A, Leaf flattening in *pks* single mutants in wild type and *nph3* sensitized backgrounds. Plants were analysed as in Figure 1A. B, Western blot of protein extracts from wild type (WT), *pks2-1* and *pks2-2* plants probed with anti-PKS2 and anti-DET3 (loading control) antibodies. A truncated form of PKS2 is present in low amounts in the *pks2-1* allele (arrow). No signal could be detected in *pks2-2* plants. Consistent with this observation is that the *pks2-2* allele produced stronger epinasty phenotyes than the *pks2-1* allele. C, Visual comparison of leaf epinasty in *nph3pks* mutants. Plants were grown for 44 days under 150 µmol.m^{-2}.s^{-1} at 20°C with a 16 hours light photoperiod. Note that beyond a certain severity of leaf epinasty (e.g. *nph3pks1pks2*) the leaves tended to curl on the soil surface. Scale bare = 2 cm.

Figure S2

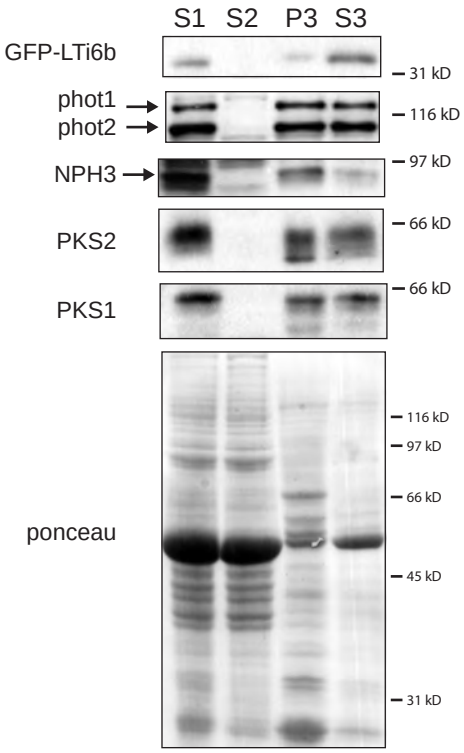

Figure S2. Co-localisation of PKS1, PKS2, NPH3, phot1, phot2 and GFP-LTi6b in insoluble protein fractions. Microsomal fractions were prepared from green tissues of 14-day-old plants (S1, total protein extract; S2, supernatant fraction after ultracentrifugation). The microsomal pellet was resuspended with 0.5% (v/v) Triton X-100 (P3, pellet after detergent treatment; S3, supernatant fraction after detergent treatment). Proteins were separated using 10% SDS-PAGE, blotted onto nitrocellulose membranes and probed with specific antibodies. GFP-LTi6b was detected using anti-GFP antibodies.

Figure S3

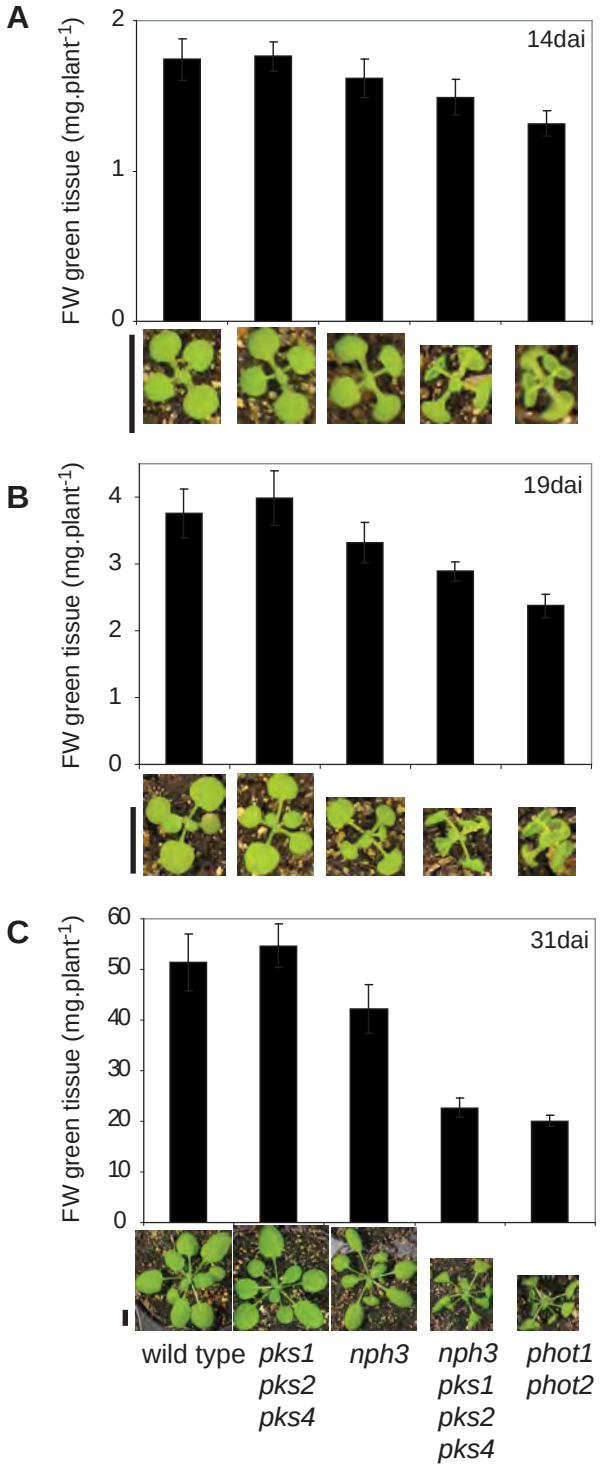

Figure S3. Growth of wild type and epinastic mutant plants under intermediate white light fluence rate. Plants were grown at 20.5 ± 1°C under 75 ± 8 µmol.m^{-2}.s^{-1} WL with a 16 hrs light photoperiod and were shuffled around to even out the effects of varying microenvironments. Fresh weight (FW) of green tissue was measured at 14 (A), 19 (B) and 31 (C) days after incubation (dai). Graphs show average values ± 95% confidence intervals for 20<n<36 plants. Lower pictures show one representative plant for each genotype. Scale bar = 1 cm.

Figure S4

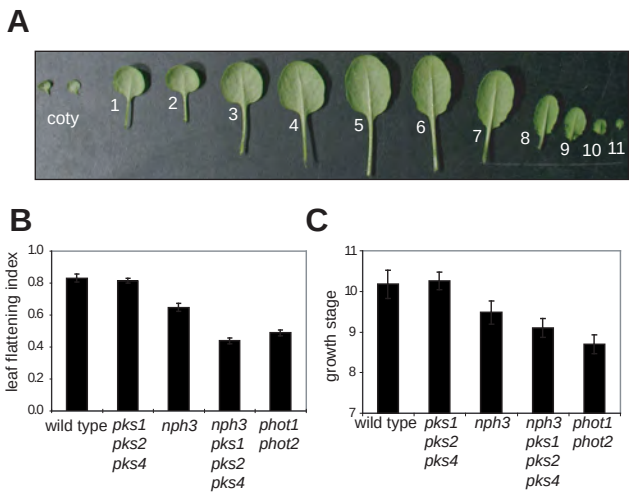

Figure S4. Morphology of leaves of wild type and epinastic mutant plants. Leaves of plants from Figure 6C were analyzed. A, Heteroblasty of a wild type plant. Cotyledons (coty) and true leaves number one to eleven (1-11) are shown. Note the difference in size and shape between juvenile (one to three), transition (four to five) and adult (six and onwards) leaves. Leaf number five appeared large and well expanded. B, Leaf flattening in wild type and epinastic mutants. Leaves were analyzed as in Figure 1. C, Growth stage reached by plants at the time when leaf number 5 was analysed. Number of the last leaf longer than 1 mm was used as an indicator of development (Boyes et al., 2001). Plots show average ± 95% confidence intervals for $20<n<36$ plants. Similar trends were found for plants grown under 75 $\mu mol.m^{-2}.s^{-1}$ (data not shown).

Figure S5

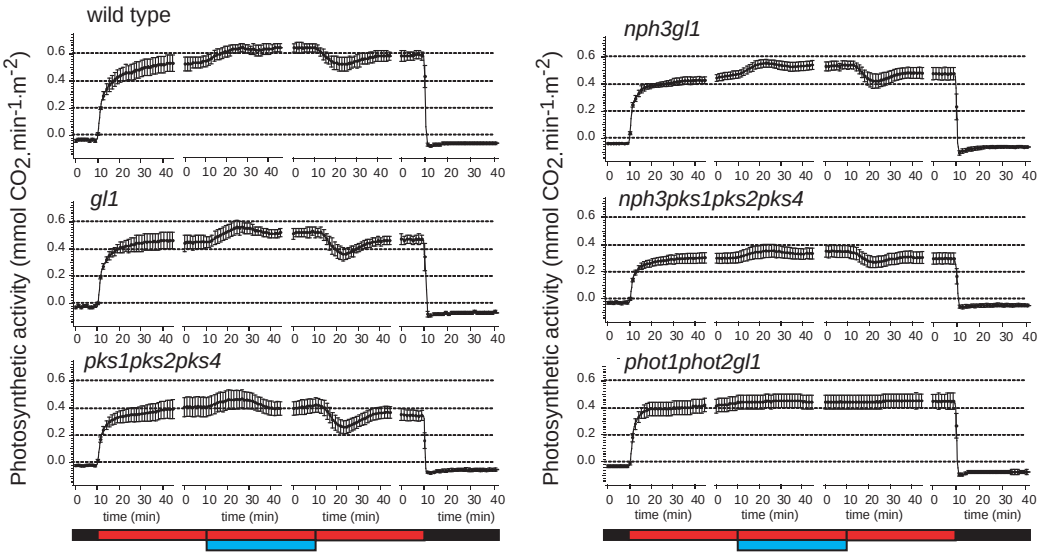

Figure S5. Epinastic leaves are impaired in photosynthetic activity. Plants were grown and analyzed as in Figure 7C. Leaves were dark-adapted (dark bar) then illuminated on their adaxial side with 500 µmol.m^{-2}.s^{-1} RL (red bar) and 25 µmol.m^{-2}.s^{-1} BL (blue bar) on a 21 mm-wide stretch approximately 5 mm from the apex of the leaf. Gas exchange was measured on the abaxial side over time. Graphs show average ± SE of 5<n<9 plants.

Figure S6

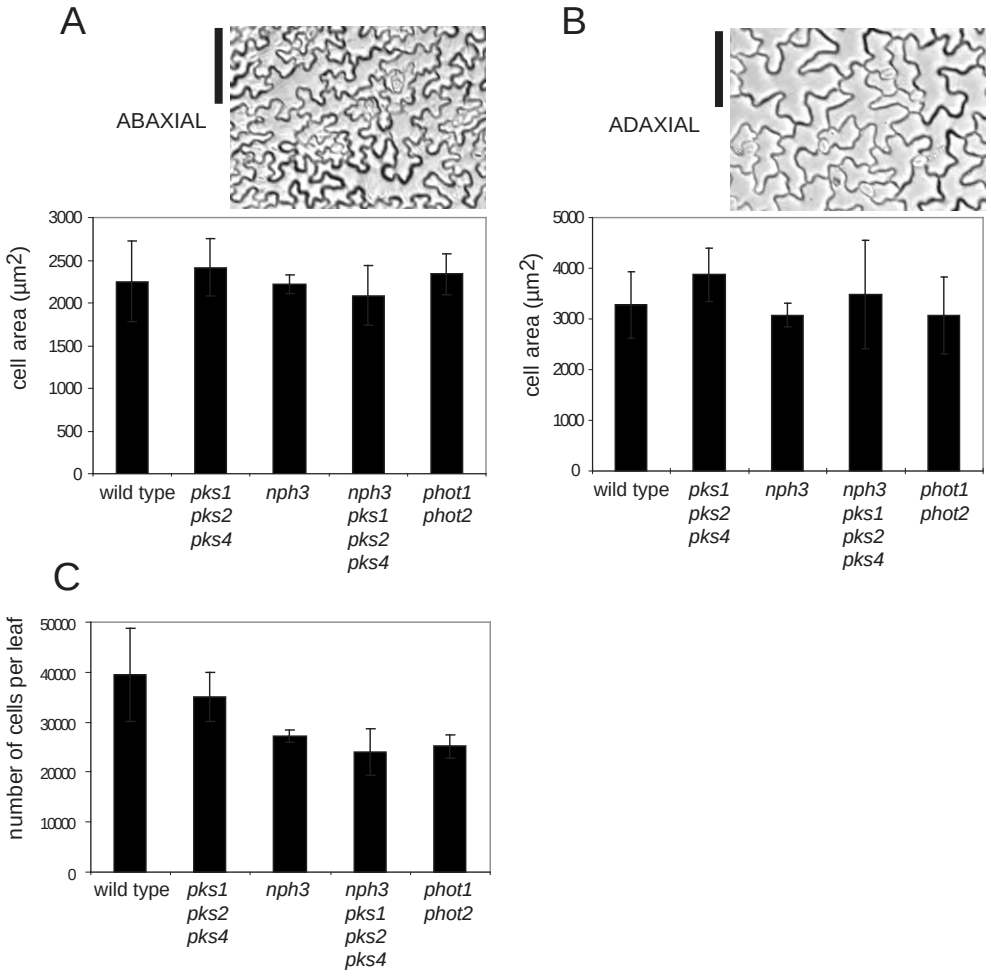

Figure S6. Analysis of epidermal cells in wild type and epinastic plant. Plants grown as in Figure 1. Epidermal prints were obtained using nail polish and observed under 100 × magnifications. Cell size was determined by measuring the area of a region comprising 60-120 cells and dividing this area by the number of cells. Plots show average ± SD for five leaves. Different regions per leaf (margin to mdivein, apex to base) were analyzed.
(A) Cell size on abaxial epidermis of leaf number 5.
(B) Cell size on adaxial epidermis of leaf number 6.
(C) Number of cells per leaf number 5. Values are the product of the total leaf area measured as in Figure 1 (mm^2) with the epidermal cell density (mm^{-2}).
Scale bar = 100 µm.